1-1-2018

Role Of The Rna Modification N6-Methyladenosine In Normal Hematopoiesis & Disease

Radovan Vasic

Role of the RNA Modification N6-methyladenosine in Normal Hematopoiesis & Disease

A Thesis submitted to the
Yale University School of Medicine
in partial fulfillment of the requirements for the
Degree of Doctor of Medicine

by
Radovan Vasic
YSM 2018

Abstract

Role of the RNA Modification N6-methyladenosine in Normal Hematopoiesis & Disease. Radovan Vasic, Yimeng Gao, Yuanbin Song, Toma Tebaldi, Stephanie Halene. Section of Hematology, Department of Internal Medicine, Yale University School of Medicine, New Haven, CT.

N6-methyladenosine (m^6A) is the most abundant modified nucleotide occurring in mRNA, with key roles in RNA metabolism and regulation of gene expression. Proposed effects of m^6A modification of RNA transcripts include effects on transcript half-life, translation efficiency, splicing and miRNA biogenesis. Importantly, m^6A is the only known dynamic RNA modification, with deposition mediated by the "writer" METTL3, and demethylation carried out by the "erasers" ALKBH5 and FTO. We hypothesized a role for m^6A in hematopoiesis, with potential disease relevance in myeloid malignancies.

To gain an understanding of the effects of m^6A on normal hematopoiesis and myeloid malignancies such as the myelodysplastic syndromes (MDS) and acute myeloid leukemia (AML), we developed conditional knockout mice for the m^6A writer METTL3, and the eraser ALKBH5. We find that deletion of METTL3 results in embryonic lethality, with an accumulation of dysfunctional hematopoietic stem cells (HSCs) that are incompetent in hematopoietic rescue assays. We further characterize disturbances in myeloid & lymphoid lineage differentiation. Deletion of ALKBH5 does not result in steady-state hematopoietic dysfunction, but results in hematopoietic stem cell deficiencies in competitive transplant assays.

We propose that deletion of METTL3 locks HSCs in a naïve multipotent state, and hypothesize that ALKBH5 exerts effects on HSC function that are yet to be characterized.

Acknowledgements

This thesis is the product of a tremendous amount of guidance, instruction and support from many individuals.

Firstly I would like to provide my thanks to Dr. Stephanie Halene, whose mentorship has been invaluable during the past five years. She has fostered my competence and independence as an aspiring physician-scientist, and supported and facilitated the development of this project.

Second I would like to acknowledge the contributions of the many member of our laboratory who participated in this project. Many of the mouse experiments presented below were performed with Yimeng Gao who has been a partner and a mentor in this endeavor. Experimental assistance and training was provided by Yuanbin Song. Anastasia Ardasheva assisted with the experiments. Toma Tebaldi performed the bioinformatic analysis.

I would also like to acknowledge other members of the lab who have been influential: Ashley Taylor and Poorval Joshi, for their patience in training me in laboratory techniques; Kunthavai Balasubramanian, for her kind demeanor and willingness to help, and Stephen Liang for his mentorship during my prior projects in the laboratory.

This work was financially supported by the American Society of Hematology Physician-Scientist Career Development Award and the William U. Gardner Memorial Student Research Fellowship at the Yale School of Medicine.

Table of Contents

Introduction

The Myelodysplastic Syndromes

The myelodysplastic syndromes (MDS) encompass a variety of disorders characterized by clonal hematopoiesis and differentiation defects in the myeloid lineage. Clonal hematopoiesis refers broadly to the outgrowth of a single hematopoietic stem cell (HSC) and its progeny as a consequence of a competitive growth advantage endowed by disease-causing mutations. The advantaged stem cell clone displaces the remaining normal HSCs, while giving rise to abnormal myeloid precursors which cannot successfully navigate myeloid differentiation. This results in an accumulation of stalled, immature myeloid "blasts" in the bone marrow, with a scarcity of mature myeloid cells in the peripheral blood[1–3]. Clinically, insufficient numbers of erythrocytes produce anemia & fatigue, decreased numbers of leukocytes result in immunocompromise & infection, and depleted or dysfunctional platelet reserves coincide with easy bruising and hemorrhage.

The number of lineages affected by peripheral blood cytopenias, as well as the frequency of myeloid blasts in the bone marrow form the basis of the WHO clinical classification of MDS. The various subtypes of MDS reflect a spectrum of disease ranging from mild cytopenias to overt acute myeloid leukemia (AML). Refractory cytopenias with unilineage dysplasia or multilineage dysplasia (RCUD, RCMD) are both characterized by fewer than 5% blasts in the bone marrow, while refractory anemia with excess blasts (RAEB I & II) encompasses two subtypes of increasing severity, with 5-9% marrow blasts and 10-19% marrow blasts, respectively. Additional subtypes are specified by hallmark features, such as the presence of ringed sideroblasts (refractory anemia with

ringed sideroblasts; RARS), monocytosis (chronic myelomonocytic leukemia; CMML), or association with genetic deletion of 5q (MDS with isolated 5q-). prevention of hematologic neoplasms or early disease therapy[2,4].

Of note, MDS is a disease of older patients, with a median age at diagnosis of 71 years. Disease morbidity and mortality are high [4,5], and therapeutic options are limited. Typically, patients with MDS are managed based on the number and severity of peripheral blood cytopenias. Patients with low risk disease or favorable prognosis can continue with a regimen of supportive care including transfusions, antibiotics, and growth factor replacement with erythropoietin or granulocyte-stimulating factors. Select patients may respond to immunomodulatory therapy with antithymocyte globulin, thalidomide or lenalidomide[6]. Patients with presence of the chromosomal lesion del(5q) are similarly responsive to lenalidomide[6,7]. For patients with high risk disease, DNA hypomethyalting agents such as decitabine or 5-azacitidine are used, though their mechanism of action is poorly understood. Though azacitidine prolonged survival by several months in clinical trials, overall survival remained poor at approximately 2 years[8,9]. Treatment with decitabine produces similarly modest results[10]. Allogeneic stem cell transplant remains the only curative option for MDS, but its use has been limited to young patients with higher risk disease[11].

Though these therapies are useful and important tools in the face of a tremendously poor outcomes, they do little to specifically target disease pathogenesis, and the basic mechanisms underlying MDS remain incompletely understood. Insights into the genetic lesions and consequent altered cellular processes in MDS have been of

particular interest, as they could serve as prognostic markers of disease, and potential therapeutic targets.

The Spectrum of Clonal Hematopoiesis

Importantly, MDS exists as one of a broad spectrum of clonal disorders affecting the myeloid lineage which share common underlying pathophysiology and mutations. On the more severe end of this spectrum lie the acute myeloid leukemias (AML). Approximately one third of patients with MDS will have their disease progress to a 'secondary' acute myeloid leukemia (sAML). By clinical criteria, patients are considered to have progressed when the frequency of bone marrow blasts exceeds 20%[1,2]. While this threshold is somewhat arbitrary, increasing blast percentage in the bone marrow coincides with their emergence in the peripheral blood. As immature blasts flood the peripheral blood, the transformation to leukemia is reflected in laboratory testing by an increasing leukocyte count on laboratory testing. While AML may arise secondary to MDS as described, the majority of AML arises *de novo*, without any apparent precursor condition. The disease-causing mutations occurring in *de novo* AML overlap with those observed in sAML, but their distribution diverges significantly a subset of mutations diverge significantly. Splicing factor mutations, for instance, tend to occur preferentially in sAML, while NPM1 mutations are characteristic of *de novo* AML[12]. This suggests some distinction in the disease mechanisms of these two conditions.

While acute leukemias reflect the most aggressive end of the spectrum of clonal hematopoiesis, a 'clinically-silent' variant termed clonal hematopoiesis of indeterminate potential (CHIP) has also recently been described[13]. The discovery of this condition was driven by the hypothesized existence of a precursor condition to both MDS & AML that

might be detected in healthy individuals. In theory the accumulation of only one or two disease-causing mutations in a hematopoietic stem cell would provide it with a competitive growth advantage over neighboring HSCs. This would result in an expansion of the mutant clone, without manifesting as overt malignancy. Over time, the accumulation of additional mutations in these pre-malignant HSC clones might lead to the development of overt MDS or AML. Importantly, this hypothesized period of benign clonal hematopoiesis in healthy individuals would provide a window of time during which early hematopoietic neoplasia could be detected and eradicated prior to the development of malignancy.

The existence of such a condition was recently substantiated by deep sequencing of peripheral blood samples from large observational trial cohorts[14,15]. While none of the individuals in these trials had any known hematopoietic disease, sequencing revealed low-frequency accumulation of mutations associated with MDS & AML in 10-20% of the study population. These individuals typically carried only one or two MDS mutations, with expansion of the hematopoietic clone inferred from increased mutant allele frequency[14]. This observation has formed the basis for a working formal definition of CHIP – patients with CHIP must have somatic clonal mutations affecting genes associated with hematologic malignancy in the absence of any clinical or laboratory evidence hematologic malignancy, with a mutant allele frequency exceeding 2% in the peripheral blood[12]. Like MDS and AML, CHIP tends to occur in older individuals, reflecting the increasing stochastic mutation burden with age. Nevertheless, there are also individuals with CHIP as young as 40 years of age[14,15]. The extent to which CHIP fulfills the role of hypothesized precursor condition to MDS or AML is somewhat limited. In

general, few cases of CHIP transition to MDS or other hemaopoietic malignancies, totaling only 0.5-1% risk of progression per year[14]. As a result, though CHIP exists along the same spectrum of myeloid disease pathophysiology as MDS and sAML, it is exceedingly more likely that CHIP will occur as a standalone condition in elderly individuals without progressing.

With this in mind, study has turned towards other possible non-malignant, chronic effects of this condition. Surprisingly, CHIP has been tied to increased mortality related to atherosclerotic coronary artery disease, with dysfunctional granulocytes and macrophages proposed to contribute to enhanced inflammation and atherosclerotic plaque formation[15]. This altogether unexpected finding ties the realm of hematologic neoplasm to cardiovascular mortality.

While these studies have successfully identified a new disease entity with unexpected clinical outcomes, the limited progression of CHIP to MDS or AML suggest that CHIP is unfortunately not likely to be a meaningful point of intervention for broad prevention of hematopoietic malignancy. As a result, the study of disease mechanisms in MDS remains an important endeavor towards developing therapies and minimizing the disease burden of myeloid malignancies.

Disease Mutations in MDS

Recent efforts to characterize MDS have focused on deep sequencing and mutation discovery. Sequencing cohorts of MDS patients has led to the identification of recurrent mutations in genes involved in epigenetic regulation (TET2, IDH1/2, DNMT3A, ASXL1, EZH2), signal-transduction (JAK2, MPL), the RAS & p53 pathways, cohesin complexes, known hematopoietic transcription factors (ETV6, RUNX1, GATA2)

and the RNA Splicing machinery[1,16,17]. Mutations in splicing machinery proteins – primarily SF3B1, U2AF1 and SRSF2 – occur in 65% of MDS cases overall, and 25% of sAML cases[17]. Notably, mutations in individual splice factors are mutually exclusive. Taken together, these findings imply either that these mutations funnel into a common disease phenotype, or that mutations in two or more spliceosome components are lethal[16].

Mutations resulting in altered epigenetic regulation include those occurring in IDH1, IDH2, and Tet2[18]. Mutations in IDH1/2 occur in 5-20% transformed% of patients with MDS and up to 30% of patients with de novo and secondary AML[19,20]. Cytosolic IDH1 and its mitochondrial counterpart IDH2 are responsible for the conversion of isocitrate to 2-α-ketoglutarate (α-KG) in the context of cellular metabolism. Mutations in residue R132 of IDH1, and R140 or R172 in IDH2 endow these enzymes with a neomorphic function, resulting in the conversion of α-KG to D-2-hydroxyglutarate (2-HG)[21–23]. In addition to its role as an intermediate in the citric acid cycle, α-KG is a required metabolite for the function of the α-KG-dependent dioxygenase family of enzymes. Owing to its close molecular resemblance to α-KG, 2-HG acts as a competitive inhibitor of α-KG-dependent enzymes.

Interestingly, Tet2 is an α-KG-dependent dioxygenases. Tet2 mutations are furthermore mutually exclusive with IDH1/2 mutations, implying a common function. Indeed, consistent with the hypothesized mechanism of action of 2-HG, Tet2 is inhibited in the context of IDH1/2 mutations, resulting in a DNA hyper-methylation phenotype resembling the phenotype of Tet2-mutant malignancies[20]. This suggests that alered 5-mC deposition is a common feature of IDH1/2 and Tet2 mutations that may have special relevance for malignancy.

Since the elucidation of this basic mechanism, several additional α-KG dependent dioxygenases have been implicated downstream of IDH1/2. These have included the Jmj family of histone demethylases[24], and the DNA demethylases ALKBH2 & ALKBH3[25], which are involved in DNA repair. These enzymes have been proposed to play a role in disease pathogenesis and are relevant to therapeutic vulnerabilities in IDH1/2 mutant cancers.

The Epitranscriptome: N-6-methyladenosine

For many decades, RNA bases have been known to carry various modifications. The N-6-methyladenosine (m^6A) mark is the most abundant mRNA modification and was among the first to be described[26]. Though m^6A was identified in RNA decades ago, study of this modification was limited for many years. For one, technical limitations made it difficult to extensively characterize. Detection of the modified ribonucleoside initially depended on liquid chromatography, which limited study to a handful of transcripts at a time. In addition, though a methyltransferase "writer" protein depositing m^6A had been discovered and characterized, the absence of a demethylase or "eraser" protein suggested that the modification was static once deposited. This led to the assumption that m^6A was unlikely to participate dynamically in regulation of gene expression.

Ultimately this assumption was overturned with the recent discovery that the fat mass and obesity-associated protein (FTO) catalyzes the demethylation of m^6A [27]. This was followed shortly by the discovery of a second demethylase, ALKBH5 [28]. Interestingly, both demethylases are α-KG dependent dioxygenases. The discovery of demethylases introduced the possibility that physiologic gene regulation might be

mediated by m^6A at the level of the transcript, a concept that reinvigorated interest in the possibility of a dynamic "epitranscriptome". Simultaneously, technical advances made it possible to study the transcriptome-wide distribution of m^6A. Using an antibody specific for the modified m^6A nucleotide, RNA transcripts containing could be selectively immune-precipitated and fragmented prior to RNA sequencing, with the location of modified m^6A modified bases inferred from the sequencing peaks. This process, termed m^6A-seq or methylated RNA immunoprecipitation and sequencing (meRIP-seq) by independent groups[29–31], provided the first insights into the distribution and function of m6A nucleotides.

The Epitranscriptome Map

The first two transcriptome-wide maps of m^6A were published within months of each other with largely convergent results[29,30]. In both cases, human and murine tissues were subjected to m^6A seq, with ~13,000 m^6A peaks identified within ~8,000 gene coding transcripts and several hundred non-coding transcripts. Overall, 95% of m^6A sites was intragenic. The observed m^6A peaks conformed to the expected RRAC (R = purine) consensus motif, which is identical to the binding motif of the previously identified m^6A methyltransferase METTL3. In both studies, the distribution of m^6A across the transcription start site (TSS), 5'UTR, coding sequence (CDS), and 3'UTR was examined.

The most prominent feature of the m^6A distribution was its heavy enrichment in the 3'UTR near the stop codon. The 3'UTR and region adjacent to the stop codon accounted for over a quarter of all m^6A residues, representing a greater than two-fold enrichment when normalized for length, and one third of all genes contained an m^6A site in these regions.

While the TSS was also relatively enriched for m^6A, many of these sites did not conform to the expected consensus sequence, leading to the conclusion that these sites were likely false positives owing to antibody recognition of the similar (N^6-,2'-O)-dimethyladenosine (m^6A_m) modified nucleotide. The first base nucleotide downstream of the 5' m^7G cap of mRNA undergoes constitutive 2'-hydroxymethylation of the nucleotide ribose – as a result, when the first incorporated nucleotide is m^6A, m^6A_m results. Several subsequent studies confirmed that the enrichment of 'm^6A' in the 5'UTR is, in fact, attributable to m^6A_m[32–34].

The CDS contained the most m^6A peaks of any region, but was relatively under-enriched when normalized for length. There was a strong tendency for increasing m^6A deposition towards the 3'end of the CDS[29,30].

Beyond mapping the distribution of m^6A, both groups provided evidence towards its potential function.

To show that m^6A might be dynamically modified, m^6A-seq was performed on human hepatocellular carcinoma cell lines under a series of stress conditions including UV light, heat shock, growth factor & interferon signaling. While 70-95% of peaks were conserved across all conditions, a subset of m^6A sites were altered in each case suggesting physiologic adaptability under stress conditions[30].

Using computational algorithms to identify RNA regulatory elements associated with the m^6A motif, one group showed that m^6A motifs overlap with miRNA binding sites in the 3'UTR, suggesting possible regulation of m^6A-modified transcripts by miRNAs[29].

Both groups explored the possibility of m^6A mediated splicing, but reached opposing conclusions. While knockdown of METTL3 appeared to produce differential splicing in hepatocellular carcinoma cell lines[30], computational motif recognition of m^6A sites did not find any significant enrichment at exon-exon junctions, which would presumably be required for differential splicing factor recruitment.

Lastly, to identify mediators of downstream effects of the m^6A modification, one of the groups used RNA affinity chromatography with and m^6A-containing bait transcript to identify the first known "readers" of m^6A including the YTH family proteins YTHDF1, 2 & 3.

These findings provided the first evidence for a dynamic epitranscriptome mediating transcript-level regulation of gene expression. Since the publication of these landmark studies, an abundant literature has emerged characterizing the role of m^6A in molecular, cellular and organismal processes. This has coincided with an expansion of the known repertoire of m^6A interacting proteins. In addition to the aforementioned erasers (FTO & ALKBH5), new components of the methyltransferase complex (METTL3, METTL14, WTAP, RBM15) and several novel m^6A "readers" (YTHDF1, YTHDF2 YTHDC1, eIF3, hnRNPA2B1, HUR) have been identified. As this literature has evolved, many of the initially hypothesized roles for m^6A and its interacting proteins have been further revised or contextualized.

Here, I will provide a brief review of the emerging m^6A literature, provide the rationale for a hypothesized role of m^6A in hematopoiesis in myelodysplasia, and discuss some of the recent evidence supporting a role for m^6A in human malignancy.

Hypothesized Role of m^{6}A in Hematopoiesis

The possibility of a role for the m^{6}A machinery in hematopoiesis is compelling. Both known erasers of the m^{6}A mark – FTO and ALKBH5 – are members of the family of α-KG-dependent dioxygenases[27,28]. The α-KG-dependent dioxygenases have previously been implicated in the pathogenesis of IDH1/2-mutated MDS & leukemia, as discussed above. It is possible that IDH mutations lead to a similar, 2-HG mediated inhibition of the α-KG-dependent dioxygenases. While this observation formed the initial basis for our interest in m^{6}A during hematopoiesis, in the time since we have initiated our own studies, several studies have been published demonstrating the relevance of m^{6}A to the pathogenesis of IDH1/2 mutant AML[35–37]. Elsewhere, several groups have observed that METTL3 is overexpressed in AML in comparison to normal hematopoietic cells[38–40]. Lastly, RBM15 (also known as OTT1), a component of the methyltransferase complex that guides it to specific target sequences[41], is a component of the fusion oncogene OTT-MKL, which occurs in acute megakaryoblastic leukemia[42]. These findings will discussed further below.

Technical Advances in the Detection of m^{6}A

Since the development of the initial m^{6}A-seq protocol, several improvements on the technique have been made. The m^{6}A-seq protocol relies on fragmentation of RNA to ~100-200 nucleotide fragments, followed by immunoprecipitation of the modified RNAs with an m^{6}A-specific antibody. The m6A-enriched RNA is then competitively eluted from the antibody, followed by cDNA synthesis and traditional high-throughput sequencing. The major limitation of this technique is the level of resolution – because of the size of the input RNA fragments, the sequencing reads inevitably form a broad peak

flanking the isolated m^6A site. Because of the relative frequency of the RRAC motif, which could occur every 64 nucleotides, a single sequencing peak can encompass more than one consensus motif[31]. This would preclude identification of the precise location of an m^6A site. Furthermore, this would preclude identification of modified adenosines occurring outside the pre-determined consensus motif.

Improved resolution of m^6A identification has been achieved by combining m^6A-specific immunoprecipitation with crosslinking and immunoprecipitation (CLIP), a well-established technique typically used to identify the target sites of RNA-binding proteins.

In traditional CLIP, protein crosslinking to bound RNA is induced via UV irradiation. The protein of interest is then immunoprecipitated, and then the bound RNA is digested to ~30-70nt fragments labeled with radioactive Phosphorus-32 (P32), and tagged with sequencing adapters. Radioactive protein-RNA complexes are then isolated by SDS-PAGE electrophoresis, and the bound protein is removed by Proteinase K digestion. The isolated RNA can then be reverse transcribed to cDNA, which is submitted for high-throughput sequencing. Binding sites can be inferred from the resulting distribution of sequencing peaks, as would be possible in m^6A-seq. Howe, crosslinking also produces artefacts in the sequencing data which identify the crosslinking site at single-nucleotide resolution. UV irradiation leads to hallmark crosslink-induced mutation sites (CIMS). Reverse transcription is also often prematurely truncated by a residual polypeptide fragment attached to the RNA following proteinase K digestion, which result in the formation of crosslink-induced truncation sites (CITS)[43]. An improved variant of CLIP termed termed individual-nucleotide CLIP (iCLIP) relies on the circularization of cDNA products to position CITS directly downstream of a

transcript-specific barcode sequence. These circularized cDNAs is then linearized by cleavage at a specific restriction enzyme digest site, and sequenced, allowing for identification of CITS at the first nucleotide position downstream of the crosslink site[44]. Ultimately these characteristic alterations can be detected computationally, and assembled into reliable RNA-binding maps.

Performing m^6A-directed iCLIP (miCLIP) is accomplished relatively simply by preforming the iCLIP on RNA incubated with an m^6A-specific antibody. In this instance, UV irradiation crosslinks the m^6A antibody directly to modified nucleotides prior to immunoprecipitation, allowing precise m^6A localization. Minor variations of this procedure were published within months of each other[33,45]. The initial characterization of miCLIP demonstrated that it reliably identified validated m^6A modification sites, including m^6A_m nucleotides in the 5'UTR. Furthermore, miCLIP identified m^6A on small RNAs such as snoRNAs, which are normally too small to allow reliable m^6A identification[33]. The Darnell group made the further observation that reverse transcription across m6A immunoprecipitated RNAs without crosslinking could also lead to premature truncation. By comparing the cDNA sequence derived from input RNA with cDNA derived from m^6A-IP samples, m^6A-induced truncation sites (MITS) could also be identified. They termed this combined procedure m^6A-CLIP/IP, and used it to identify m^6A sites with high confidence[45].

Importantly, these techniques resolved existing ambiguities in the epitranscriptome map. Performing m^6A-CLIP/IP confirmed the enrichment of m^6A in the 3'UTR, with over 70% of m^6A nucleotides found in this region. However, the enrichment of m6A near the stop codon was clarified[45]. CLIP directed against m^6A showed that m^6A

decreases gradually towards the 3' end of the CDS and peaks rapidly within the first 150-400 nucleotides of the last exon. Though this region tends to be closely associated with the stop codon, the precise placement of m^6A nucleotides within the 3'UTR was agnostic to the position of the stop codon. Rather, it appears that m^6A is preferentially found in the last exon. This finding was confirmed by examining a subset of RNAs which have a non-coding last exon downstream of a stop codon in a preceding exon. In these cases, m^6A methylation continued to be enriched in the last exon, without enriched methylation near the upstream stop codon. [45]. These increasingly specific findings reflect the value of enhanced resolution with m^6A-CLIP/IP & miCLIP.

To this point miCLIP represents the tool of choice for transcriptome-wide m^6A mapping. While this represents a tremendous advance, the protocol intrinsically depends on the specificity of the antibody, efficiency of immunoprecipitation and crosslinking, which are likely imperfect. Alternative methods have been used to sequence other modified nucleotides. The DNA & RNA modification 5-methylcytosine (5-mC) is identified by treatment with bisulfite, which induces characteristic mutations of 5-mC to uracil. The DNA modification N6-methyladenine (N6-mA) is identifiable by characteristic slowing of DNA Polymerase during sequencing. To date, m^6A has proved resistant to chemical modification, and produces no detectable sequencing artefacts. In the future the development of such techniques may further improve detection of m^6A.

Molecular Roles of m^{6}A: Integration of RNA Metabolism

With the technical advances in transcriptome-wide detection of m^{6}A, there has been tremendous interest in its effects on RNA metabolism. Proposed roles thus far have included effects on transcript stability, translation efficiency, alternative splicing, polyadenylation, and recruitment of RNA binding proteins. In the subsequent sections I will discuss the effects of m^{6}A RNA biology at the molecular and cellular levels.

Timing of m^{6}A Deposition and the "Dynamic" m^{6}A Methylome

Multiple studies provide strong evidence that m^{6}A is deposited co-transcriptionally. One of the most rigorous relied on cell fractionation techniques to specifically isolate chromatin-associated RNA (CA-RNA), nucleoplasmic RNA and cytoplasmic RNA. CA-RNA is composed predominantly of nascent pre-mRNA transcripts, which are partially spliced. By the time these transcripts reach the nucleoplasm, transcripts are fully spliced, and are finally trafficked into the cytoplasm. Performing miCLIP on these fractions in HeLa cells revealed that 90% of m^{6}A peaks are identical between CA-RNA and nucleoplasmic RNA, while over 99% are identical between nucleoplasmic and cytoplasmic RNA[46]. These results provide strong evidence that the overwhelming majority of m^{6}A must be deposited co-transcriptionally. Of note, the minor differences between nucleoplasmic and cytoplasmic RNA methylation also call into doubt the extent to which the predominantly nuclear m6A erasers FTO and ALKBH5 perform meaningful RNA demethylation in steady-state conditions[47].

Additional evidence for co-transcriptional RNA modification comes from the detection of METTL3 bound to chromatin-associated nascent RNA transcripts. In modified chromatin immunoprecipitation (ChIP) experiments, METTL3 bound to

elongating RNA transcripts can be detected by long-range chemical crosslinking of proteins to the associated DNA upon treatment with disuccinimidyl glutarate. This procedure demonstrated that the methyltransferase complex is bound to nascent RNA in close association with chromatin throughout the genome, in a distribution reminiscent of the known m^6A methylome. Performing ChIP against METTL3 during heat shock further revealed a global reduction in METTL3 binding with specific re-localization to heat shock genes[48]. In another study, traditional ChIP directed against METTL3 in AML cell lines demonstrated that METTL3 can also be recruited to the promoters of genes whose transcripts are subsequently m^6A-modified[38].

Together these findings support early deposition of m^6A during transcription. The consistent m^6A distribution across nuclear and cytoplasmic RNAs strongly suggests that the RNA demethylases FTO & ALKBH5 may not exert a significant influence on steady-state RNA metabolism. However, this finding needn't imply that m^6A cannot be 'dynamically' modified. The redistribution of METTL3 upon heat shock implies a distinct mechanism of inducing global shifts in m^6A profile[48]. Similarly, experimental modulation of FTO expression during heat-shock suggests its important regulatory function in stress-response[49]. The m^6A readers, writers, or erasers may be similarly induced during stress conditions, cellular signaling, or developmental events to remodel the m6A methylome.

Effects of m^{6}A on Transcript Stability & Translation Efficiency

The effects of m^{6}A on RNA metabolism following transcription has been investigated at the level of transcript stability and translation efficiency using a straightforward set of molecular techniques.

Transcript abundance is readily determined by traditional RNA-sequencing, while m^{6}A modified transcripts may be identified via miCLIP.

The ***half-life of transcripts*** can be assessed by RNA sequencing at multiple time points following treatment with the transcription inhibitor actinomycin D. In theory, with no new transcripts entering the cellular pool of RNA, transcript decay can be measured in this manner. This procedure has been termed RNA lifetime profiling.

Lastly, effects of m6A modification on ***ribosomal loading*** and ***efficiency of translation*** can be determined by ribosome profiling (also known as ribo-seq, or ribosome footprinting). In this technique, ribosomes are locked in place on actively translated mRNAs by treatment with the translation inhibitor cycloheximide. Ribonuclease treatment degrades exposed mRNA, while the immobilized ribosomes protect their bound mRNA fragments. The ribosome-bound mRNAs can then be isolated using size-specific protein isolation techniques such as sucrose gradients. The intact mRNAs are then dissociated from the ribosomes and can then be subjected to traditional RNA sequencing[50]. The quantity of sequencing reads provides a measure of ribosome occupancy for a given transcript, which is used as a surrogate measure of net translation. The 'translational efficiency' of any given transcript can then be determined as a ratio of ribosome occupancy (reads per million by ribo-seq) to transcript abundance (reads per

million by RNA-seq)[51]. Several publications have leveraged these techniques to explore m^6A-mediated regulation of transcript decay and translation.

The effects of m^6A on transcript stability and turnover were first elucidated by knock-down experiments examining the function of the m6A reader YTHDF2[52]. RNA-seq and half-life profiling performed in YTHDF2 knock-down cell lines showed an increase in the abundance and half-life of m^6A-modified transcripts that were also known targets of YTHDF2. Ribosome profiling, however, showed no change in the amount of ribosome-bound mRNA in the knock-down condition. Together, these findings suggest that in the absence of YTHDF2, there must be an increase in non-ribosome mRNA in the cells. This implies that YTHDF2 promoting the degradation of m^6A-modified transcripts under normal conditions. Indeed, YTHDF2 was found to be necessary for targeting m^6A-modified transcripts to processing bodies (P bodies), which are cytoplasmic protein-RNA complexes responsible for mRNA degradation[52]. While these findings provided a clear mechanism for YTHDF2-mediated degradation of m^6A-modified transcripts, it is important to note that these experiments focused solely on the role of YTHDF2 in m^6A metabolism. The overall effect of m^6A on transcript metabolism, however, depends on the integrated effects of multiple m^6A readers. The net effect of m^6A is therefore better assessed by knocking out the methyltransferase METTL3.

Many of the early studies on METTL3 knockdown[53,54] and knockout[51,55] cells were performed on murine embryonic stem cells (mESCs). The most detailed of these examined the effects of METTL3 knockout on the early transition of mESCs from an early “naïve” state favoring self-renewal, to a “primed” state favoring differentiation referred to as epiblast stem cells[51]. In a molecular screen, METTL3 knockdown resulted

in destabilization of primed epiblast stem cells, favoring the naïve state instead. METTL3 knockout mESCs were found to be correspondingly deficient in hallmark assays of tri-lineage differentiation, but maintained enhanced self-renewal activity even after recovery from long-term culture in differentiation media or *in vivo* teratoma-formation assays. In keeping with these findings, METTL3 knockout mice were embryonic lethal at an early stage of development, with prolonged expression of pluripotency factors and failure to form the epiblast. These findings implied a failure to progress past naïve pluripotency.

At the molecular level, detailed analysis of METTL3 knockout mESCs demonstrated increased transcript abundance and half-life of m^6A-modified pluripotency genes in knockout mESCs, suggesting that m6A is required for the degradation of pluripotency genes[51]. These findings were accompanied by a global tendency towards stabilization of m^6A-modified transcripts, in agreement with the results of the previously discussed YTHDF2 knockdown experiments[52]. An independent study evaluating existing sequencing of mESCs similarly showed that m^6A-modified transcripts had half-lives that were up to 2.5 hours shorter than unmodified ones[55]. The decreased stability of m^6A transcripts appears to be a generalizable trend across multiple contexts, as similar effects have been observed in the context of METTl3 depletion experiments in murine embryonic fibroblasts[32], T cells[56], mouse brain[57], and HeLa cells[58]. Taken together, these experiments strongly support a global role for m^6A in promoting transcript degradation, while also demonstrating the relevance of this molecular process to stem cell biology and cell fate decisions.

While the aforementioned experiments provide evidence for m^6A-mediated destabilization of transcripts, it is important to note that decreased transcript abundance

does not necessarily imply decreased protein expression. Dramatically enhanced translational efficiency might still paradoxically result in enhanced overall protein expression even in the context of a a diminished transcript pool. Indeed, isolated knockdown of the m^6A reader YTHDF1 in HeLa cells results in decreased ribosomal occupancy of its m^6A-modified targets without any corresponding changes in transcript abundance. This implies that the YTHDF1 normally functions to enhance the translational efficiency of a fixed transcript pool[59]. To address the apparent contradiction between the mRNA degradation effects of YTHDF2 and the translation-enhancing effects of YTHDF2, Wang *et al.* used a protein tethering assay in which the functional domains of YTHDF1 and YTHDF2 were fused to a small peptide, which could in turn bind to a specific RNA element in the 3'UTR of a luciferase reporter mRNA construct. These experiments confirmed that tethering of only YTHDF1 to the reporter increases translational efficiency while tethering of only YTHDF2 promotes transcript degradation. Simultaneous tethering of both reader proteins, leads to both a sharp peak in overall protein expression as well as enhanced transcript degradation. In theory, this mode of gene expression regulation would be ideal for rapidly induced bursts of protein expression, which can be rapidly silenced at the level of the transcript. Wang *et al.* speculated that this may be relevant during cellular differentiation events, responses to physiologic stimuli, and may serve to limit noisy gene expression[59].

While the above findings demonstrate a role for 3'UTR m^6A in the regulation of translation, an independent mechanism of translation-regulation was described for m^6A occurring in the 5'UTR. Translation initiation typically requires the formation of a 43S pre-initiation complex, which consists of the 40S ribosomal subunit and eukaryotic

initiation factors (eIF1-3). These components are recruited to the 5' mRNA cap by the eIF4F complex, whose subunits achieve the combined function of binding the 7-methylguanine (m^7G) cap, and directing 43S assembly by binding to eIF3[60]. However, in cellular stress conditions such as heat shock, the necessity of the 5' mRNA cap can be bypassed to allow for 'cap-independent' translation. A series of in vitro translation experiments demonstrated that m^6A-modified transcripts can bypass the requirement of the 5' m^7G mRNA cap nucleotide and the eIF4F complex. Cap-independent translation could be induced by the addition of a single m^6A nucleotide anywhere within the 5'UTR, but not by m^6A in the CDS. Reasoning that m^6A must directly recruit one of the 43S preinitiation components to the 5'UTR, Meyer *et al.* performed protein-crosslinking experiments and identified eIF3 as an m^6A-binding protein. Transcriptome-wide profiling confirmed significant overlap of eIF3 with m^6A binding sites in the 5'UTR. Lastly, they substantiated the physiologic relevance of this phenomenon by showing that knockdown of the FTO eraser could increase 5'UTR m^6A content and mediate increased cap-independent translation during heat shock[60].

An independent study further examined the distribution of m^6A, FTO & YTHDF2 during heat shock. In this study, heat shock resulted in an isolated increase in m^6A methylation at the 5'UTR, with some specificity for heat shock transcripts. The shift in the m^6A methylome coincided with relocation of YTHDF2 from the cytosol to the nucleus. Knockdown of YTHDF2 produced a specific loss of 5'UTR methylation and decreased expression of heat shock transcripts, suggesting its necessity during heat shock. In contrast, knockdown of FTO replicated the enhanced 5'UTR methylation observed in heat shock. These findings led to the hypothesis that during heat-shock, YTHDF2 binds

to 5'UTR m^6A nucleotides and protects them from demethylation by FTO[49]. This would correspondingly lead to cap-independent translation and increased expression of heat-shock genes. This model was supported by in vitro competition assays, and by the effects of YTHDF2 & FTO knockdown on 5'UTR methylation and translational efficiency of heat-shock transcripts[49]. Together with the description of eIF3 as an m^6A reader, these two studies provide a detailed, integrated mechanism of action for the m^6A machinery in heat-shock induced cap-independent translation.

While both of these studies initially described heat shock induced cap-independent translation to m^6A, it is important to note that the enrichment of m^6A in the 5'UTR is now thought to be attributable to the dimethylated m^6A_m nucleotide. The specific pattern of enhanced 5'UTR methylation upon FTO knockdown made the original authors of the preceding publications suspicious that its true substrate was m^6A_m, rather than m^6A. They subsequently showed that FTO has a several-fold higher degree of affinity toward m^6A_m, interacts specifically with m^6A_m in the context of the 5' cap, and preferentially demethylates m^6A_m compared to m^6A in a variety of assays[61]. These findings revise the role of FTO, and imply that at least some of the role of the m^6A machinery in cap-independent translation and heat shock are attributable to m^6A_m. Notably, m^6A_m in the 5'UTR also exhibits distinct effects on transcript stability, as transcripts with m^6A_m tend to be protected from degradation by the decapping enzyme DCP2[34].

In summary, m6A exerts complex, varying effects at the level of transcription and translation. Evidence drawn from a variety of contexts strongly supports the notion that m^6A destabilizes transcripts by promoting degradation. This is certainly the case for

targets of YTHDF2, which are targeted to P bodies, where RNA degradation occurs[52]. It remains to be seen whether additional readers besides YTHDF2 function regulate the transcript stability of m^6A modified transcripts, though results from METTL3 knockout experiments suggest that the majority of methylated transcripts tend to be downregulated transcriptome-wide[51,55,56]. Notably m^6A_m in the 5'UTR protects transcripts from decapping and degradation[34].

At the level of translation, YTHDF1 enhances translational efficiency of methylated transcripts bearing m6A in the CDS or 3'UTR. Methylation at the 5'UTR promotes cap-independent translation by direct assembly of the 43S preinitiation complex via recruitment of eIF3. While this mechanism can be stimulated by the addition of m^6A anywhere in the 5'UTR *in vitro*[60], it may be predominantly mediated by m6Am *in vivo*[34]. This mechanism mediates the cap-independent translation during the heat shock response, during which YTHDF2 re-localizes to the nucleus to protect modified nucleotides from demethylation by FTO[49]. While the YTHDF1- and YTHDF2-mediated effects of m^6A on translation appear well-defined, it remains to be seen whether additional readers mediate distinct translation effects. Of note, only ~2,500 methylated transcripts were identified as YTHDF1 targets in knockdown experiments, representing only a quarter of m^6A methylated genes[59]. When broadening the scope to all m^6A methylated transcripts, the effects of METTL3 depletion vary depending on the context. In mESCs METTL3 knockout produced a global increase in translational efficiency, however this appeared to be specific for GC-rich transcripts independent of methylation status[51]. Another analysis of sequencing data from mESCs suggests decreased translational efficiency of m^6A-modified transcripts[55], while knockout in T cells results in

no detectable effects on translational efficiency[56]. These findings suggest that there may be additional reader proteins that are likely to mediate m^{6}A-dependent effects on translation.

Interactions between m^{6}A and miRNA metabolism

Among the possible regulatory roles for m^{6}A in transcript metabolism, several interactions with the microRNA (miRNA) processing machinery have been described. The term miRNA refers to short, endogenously transcribed RNAs which bind to endogenous mRNAs via complementarity to target them for degradation by cleavage, translation repression, or deadenylation. Similar RNA-mediated regulation of gene expression are conserved across lower and higher organisms, and are broadly referred to as RNA interference (RNAi). In mammals, miRNA processing begins with the transcription of a pri-miRNA, consisting of a ~22 nucleotide-hairpin with long flanking 5' and 3' sequences. The pri-miRNA must then be metabolized by the microprocessor complex, consisting of the hairpin-binding protein DGCR8, and DROSHA, which cleaves the flanking 5' & 3' regions. This results in the formation of the pre-miRNA, which is exported to the cytoplasm, where the hairpin loop is cleaved off the pre-miRNA by Dicer, and Argonaute (Ago2), producing a double-stranded RNA duplex (dsRNA). This dsRNA then dissociates into mature single stranded miRNA, which recruits Dicer, Argonaute, and additional proteins referred to collectively as the RISC complex to mediate mRNA cleavage and degradation[62].

Whereas mammals rely on miRNAs to mediate gene expression, lower organisms such as yeast can also use the RNAi machinery to mediate co-transcriptional gene silencing by recruiting Dicer directly to nascent RNA transcripts. Surprisingly,

recruitment of the RNAi machinery to elongating chromatin-associated transcripts can also be detected in mESCs[48]. While Dicer is cytoplasmic in mammals and does not associated to chromatin, long-range ChIP for the microprocessor components DGCR8 & DROSHA shows that the microprocessor is bound to coding regions across the genome, in addition to the expected miRNA loci. In coding regions, recruitment of the microprocessor coincided with transcript degradation. This effect appears to be m^6A-mediated. METTL3 ChIP revealed a genome-wide correlation with DGCR8 binding, and METTL3 knockout led to loss of DGCR8 binding and stabilized transcript expression. This mechanism appears relevant to stress response, as heat shock resulted in recruitment of METTL3 and the microprocessors machinery to heat shock transcripts, resulting in a rapid spike in protein expression paired with a coinciding decrease in transcript half-life. This pattern of accelerated transcript with enhanced protein expression matches the expected effects of the m6A modification[59], but is importantly dependent on both METTL3 and DROSHA, demonstrating the relevance of the microprocessor to this phenotype[48].

In an additional pair of studies, m^6A and its putative reader hnRNPA2B1 were tied to traditional mammalian miRNA processing. In the first study, Alarcón *et al.* proposed that m^6A nucleotides could act as recognition sites on pri-miRNAs for the recruitment of DGCR8 and DROSHA[63]. This hypothesis was based on the enrichment of the m^6A consensus motif in miRNA sequences. METTL3 knockdown correspondingly produced decreased expression of ~70% of mature miRNAs, with an accumulation of the corresponding pri-miRNAs. Methylated pri-miRNAs were also more readily converted to pre-miRNAs *in vitro*. Recruitment of DGCR8 to miRNAs was METTL3-dependent,

though DGCR8 showed no preference for direct binding of m^6A methylated transcripts in vitro, implicating a novel intermediary reader protein[63]. The same investigators subsequently identified hnRNPA2B1 as this intermediary. hnRNPA2B1 binding sites are similarly enriched for the m^6A motif, and knockdown of this protein results in loss of miRNA expression and pri-miRNA accumulation that phenocopies the METTL3 knockout. Co-immunoprecipitation confirmed a direct interaction between hnRNPA2B1 and DGCR8[64]. Thus, hnRNPA2B1 could reasonably serve as a link between m6A deposition and recruitment of the microprocessor machinery. These findings have recently been called into question, however, as hnRNPA2B1 does not replicate the binding patterns of other readers, nor does it contain a characteristic YTH domain[65]. Others groups have also not been able to replicate the link between hnRNPA2B1 and miRNA processing[66].

Lastly, the m^6A_m modification in the 5'UTR has also been associated with resistance to miRNA degradation. As previously discussed, transcripts bearing m^6A_m are resistant to DCP2-mediated decay. Since the miRNA machinery relies on decapping for mRNA degradation, it follows that m^6A_m-labeled transcripts are protected from the RNAi machinery[34].

Regulation of RNA Splicing by m^{6}A

Given the high frequency of m^{6}A modifications, their predominant presence in mRNAs, and their enrichment in long internal exons[29,30,51] many have been quick to posit a role for m^{6}A in mRNA splicing. These findings are of interest given the preponderance of mutations in splicing factors, including SRSF2, U2AF1 and SF3B1, occurring in CHIP, MDS and AML. Given the relevance of alternative splicing in hematopoietic malignancy, it is conceivable that m^{6}A-mediated alternative splicing may play a role in normal hematopoiesis and disease

The initial experiments examining METTL3 knockdown in hepatocellular carcinoma cell lines found that "multi-isoform" transcripts – those that altered their use of alternative exons without altering overall transcript abundance – were more likely to be methylated than single isoform transcripts[30]. METTL3 knockout in mESCs was similarly reported to result in significant splicing changes[51]. The m^{6}A methyltransferase complex and erasers localize to nuclear speckles, which contain core components of the splicing machinery, supporting a potential interaction. Compellingly, depletion of the erasers ALKBH5[28] and FTO[67] were both reported to regulate the recruitment of the splicing factor SRSF2 to RNA, and SRSF2 binding sites were enriched near m6A consensus motifs[67].

With respect to readers, both hnRNPA2B1 and YTHDC1 have been proposed to interact with m^{6}A, and are well-established as splicing factors. Tandem-affinity purification experiments demonstrated that YTHDC1 interacts with several serine rich (SR) splicing factor proteins including SRSF1, 3, 7, 9 & 10, though no association with SRSF2 was found. Of these, knockdown of YTHDC1, SRSF3, and SRSF10 resulted in

significant alterations of splicing patterns. Based on additional experiments, the authors proposed that SRSF3 and SRSF10 compete for binding sites, and that YTHDC1 allows for recruitment of SRSF3 to prevent SRSF10 binding to RNA[68]. As discussed previously, there is some doubt as to the validity of hnRNPA2B1 as a direct m^6A reader.

Despite these reported findings, the notion that m^6A mediates RNA splicing has been hotly contested, particularly by Ke *et al*. As discussed previously, m^6A is deposited co-transcriptionally, and the m^6A content of transcripts is >90% identical across chromatin-associated, nuclear, and cytoplasmic fractions. While over 98% of m6A residues were observed in exons, these were not found to be enriched near splice sites by m6A-CLIP/IP. Furthermore, Ke *et al*. analyzed raw sequencing data from previous publications and could not replicate their findings regarding splicing, suggesting that the original observations may have been byproducts of the bioinformatic analysis pipeline. They also performed RNA sequencing and m^6A-CLIP-IP on previously analyzed METTL3 knockout mESCs, and found that methylated exons did not differ in their likelihood of splicing compared to unmethylated ones, as had previously been claimed[46].

Indeed, close examination of the published findings regarding YTHDC1 as an m^6A reader reveals that the METTL3, SRSF3, and YTHDC1 knockdown conditions share only 160 mutually skipped exons, suggesting fairly low overlap genome-wide[68].

Taken together, these findings provide strong evidence that m^6A is not necessary for splicing, and may play a smaller role in splicing than originally anticipated.

Cytokine Signaling & m^{6}A Interactions in T Cell Biology

Examination of the effects of METTL3 deletion in CD4+ T cells in conditional knockout mice has unearthed both a compelling biological phenotype and a new paradigm for m^{6}A-mediated regulation of gene expression in response to cytokine signaling[56].

In this study, loss of METTL3 led to a dramatic increase in the proportion of naïve CD4+ T cells, which were resistant to activation in both *in vitro* and *in vivo* assays of T cell function. In adoptive transfer experiments, knockout T cells persisted in a naïve state with minimal proliferation, activation or differentiation. RNA-sequencing and m^{6}A-profiling revealed alterations in JAK/STAT signaling, as well as stabilization of three suppressor of cytokine signaling (SOCS) gene transcripts in the knockout condition. Typically, T cell activation and differentiation in adoptive transfer models are mediated by IL-7 signaling via JAK1/STAT5, which are known to be negatively regulated by SOCS. These observations and additional experiments led to the conclusion that IL-7 signaling depends on m^{6}A-modification and degradation of SOCS transcripts. In the absence of m^{6}A, SOCS transcripts are stabilized, leading to persistent inhibition of JAK/STAT signaling, abrogation of IL-7 signaling, and persistence of naïve T cells[56]. Under this model, extracellular signaling is mediated by rapid alternations These observations point to further possible interaction points between normal hematopoiesis and the m^{6}A machinery as JAK/STAT signaling and the SOCS genes have established roles in erythropoiesis[69–71], and m^{6}A may guide cellular fate decisions in this context.

Roles for m^{6}A in Normal Hematopoiesis and Malignancy

Over the past year, evidence has begun to emerge regarding the role of m^{6}A in normal hematopoietic stem cell behavior and malignancy. Epigenetic alterations appear to be a hallmark of MDS and AML, with well-established roles for aberrant DNA and histone methylation in disease pathophysiology. To date, it appears likely that this trend extends to alterations in RNA methylation. Below I discuss the established roles for the m^{6}A machinery components in hematopoiesis and malignancy.

METTL3 in Normal Hematopoiesis

As noted before, constitutive deletion of METTL3 in mice produces embryonic lethality early during development due to defects in the resolution of naïve pluripotency. METTL3 deletion enforces the naïve state of embryonic stem cells, and does not allow them to progress to the "primed" epiblast-like state in which they are able to differentiate into mature components of all three germ layers[51].

In contrast, morpholino-based silencing of METTL3 and METTL3 mutations in zebrafish produce a profound hematopoietic phenotype, with a decreased number of HSPCs and diminished contribution to erythroid, myeloid and lymphoid lineages. Typically the emergence of early HSPCs occurs in the aortogonadomesonephros (AGM) when a subset of AGM termed the haemogenic endothelium transitions directly into HSPCs (a process called the endothelial-hematopoietic transition, or EHT). The deficiency in early HSPC formation in zebrafish corresponded with a decreased number of haemogenic endothelial cells, and Zhang *et al.* correspondingly hypothesized that loss of METTL3 inhibited the EHT. Similar to the 'locked-in' state of METTL3 knockout ESCs, the zebrafish AGM would be lock in the endothelial state. Consistent with this

theory, RNA-seq of the AGM region in the METTL3 mutant zebrafish revealed upregulation of Notch, VEGF and vascular development pathways in the METTL3 mutants, all of which maintain endothelial identity. The authors correspondingly identified m6A peaks in the *notch1a* transcript and demonstrated that while *notch1a* transcripts rapidly degraded in wildtype zebrafish, they were stabilized upon METTL3 depletion. The hematopoietic defects could notably be rescued by small molecule inhibitors of notch signaling. Cumulatively, this led the investigators to conclude that loss of m^6A in key transcripts genes such as *notch1a* lead to stabilization of endothelial identity, and inhibit EHT. [72].

METTL3 in Malignancy

Two studies have examined the effects of METTL3 knockdown in the context of human CD34+ HSPCs and AML cell lines. Using publicly available gene expression data, both groups demonstrated that METTL3 is overexpressed in AML patients samples and cell lines compared to normal hematopoietic tissues[38,73]. Furthermore, among all malignancies, AML exhibits the highest levels of METTL3 expression, suggesting the possibility of m^6A dependency in AML[73]. To this effect, CRISPR dropout screens targeted against RNA editing enzymes recurrently identified METTL3 and METTL14 as amongst the most necessary for AML cell line survival[38]. Consistent with these results, targeted knockdown or deletion of METTL3 in murine and human leukemia cell lines abrogated cellular proliferation without effects on apoptosis, and promoted differentiation of AML cells into normal myeloid cells based on flow cytometry for the mature myeloid marker CD11b[38,73]. Loss of METTL3 also resulted in decreased colony formation in semi-solid culture, and impaired engraftment in immunocompromised recipient mice.

METTL3 knockdown similarly resulted in enhanced differentiation and impaired colony formation in normal human CD34+ HSPCs[73].

These two studies investigated independent mechanisms to explain the observed effects. In one, the authors performed RNA-seq and miCLIP, which demonstrated enrichment of DNA damage, Myc and PI3K pathways amongst the differentially regulated m^6A-modified transcripts. At the protein level, METTL3 knockdown led to loss of Myc, BCL-2, and regulators of PI3K[73]. The second study significantly expanded on the known role of the methyltransferase complex by demonstrating that METTL3 directly interacts with DNA promoters in ChIP experiments. Recruitment of METTL3 to promoter regions was mediated by CEBPZ, which recognizes CCAAT motifs in DNA. METTL3 binding in promoters corresponded to m^6A modification of the associated transcripts, and enhanced translational efficiency without affecting overall transcript levels. Mechanistic studies suggested that in the absence of m^6A, translation stalls at GAN codons (N= any nucleotide), inhibiting protein level expression. The transcription factors SP1 and SP2 were both dependent on promoter-bound METTL3 for effective translation, and rescue of SP1 expression could restore expression of its downstream target Myc, reversing the cell growth defects of the METTL3 knockdown cell lines[38]. Together these findings suggest that METTL3 is required for normal HSPC self-renewal and maintenance of AML leukemogenicity, and that these effects are mediated significantly by Myc. Importantly, the observed effects in cell lines may deviate from the impact of METTL3 deletion in native hematopoiesis *in vivo*.

Interestingly, a tamoxifen-inducible murine model of METTL14 deletion was recently published. These mice demonstrated increased myelopoiesis at 11 days

following deletion, and diminished HSC engraftment in competitive repopulation assays. METTL14 was similarly shown to be upregulated in AML subtypes with specific chromosomal translocations. Myeloid transcription factors including PU.1 and CEBPA were found to be bound upstream of METTL3 in ChIP experiments using AML cells, and loss of PU.1 resulted in upregulation of METTL14. These findings implied that PU.1 normally promotes myelopoiesis by downregulating METTL14. Consistent with previous reports, Myb and Myc were identified as downstream m^6A-modified targets of METTL14 whose function was essential for leukemogenicity in AML cell lines[40].

Altogether, the general emerging consensus based on predominantly human and murine cell line data suggests that METTL3 is required for the maintenance of HSCs, and that loss of METTL3 promotes myelopoiesis. The same appears to hold true for METTL14. Results from multiple studies suggest that these phenotypes converge on Myc & Myb signaling. Notably, none of these publications remarked on significant splicing changes as a consequence of m^6A depletion, perhaps calling into doubt the extent to which m^6A acts as a regulator of alternative splicing.

Contrasting Roles of FTO in AML

As discussed previously, our initial interest in the m^6A machinery as a relevant target in AML was driven in part by the fact that both reported m^6A demethylases are α-KG dependent dioxygenases, and could therefore be implicated in the pathophysiology of IDH1/2 mutant AML. Over the past year, several studies have examined this possibility, as well as the role of FTO in non-IDH mutant AML.

Evidence implicating FTO downstream from IDH mutations was initially presented in a limited study performed in human embryonic kidney (HEK293T) cell

lines. In HEK293T cells bearing IDH mutations, m^6A content was increased, and m^6A levels could be normalized by treatment with the IDH1/2 mutant inhibitor AG221. These findings were consistent with the hypothesized 2-HG mediated inhibition of the m^6A demethylases. Furthermore, knockdown of FTO alone increased m^6A content in wildtype cells, replicating the IDH mutant phenotype. FTO knockout in IDH mutant cells, however, could not produce any further increase of m^6A, suggesting that FTO may already be functionally inhibited in the mutant condition[35]. Because these experiments were performed in non-hematopoietic tissues, no meaningful assessment of the corresponding phenotype of FTO knockdown could be performed. Furthermore, a role for ALKBH5 could not be excluded.

In another study, FTO was counterintuitively found to be overexpressed in specific IDH1/2-wildtype AML subtypes. In murine models of MLL-AF9, FLT3-ITD, and PML-RARA driven leukemia, FTO was uniformly overexpressed, while ALKBH5 was not. FTO overexpression promoted cell growth and viability, with decreased apoptosis in both murine and human AML cell lines, and enhanced leukemogenesis of MLL-AF9 murine leukemia. RNA-seq and miCLIP led to the identification of ASB2 and RARA as FTO and m6A-dependent transcripts essential to leukemogenic activity[74].

This raised a possible contradiction. While increased FTO expression was apparently essential to certain subtypes of leukemia, its proposed role in IDH mutant malignancies would be dependent on decreased FTO expression. It is presumably unlikely that both gain and loss of FTO would be leukemogenic in distinct contexts.

A resolution to this contradiction was proposed by the same group that published the role of FTO overexpression in non-IDH AML. By broadly examining the effects of 2-

HG on 27 different human leukemia cell lines, Su *et al.* suprisingly, found that 2-HG treatment led to cell-cycle arrest and apoptosis in the majority of leukemia cell lines. This observation carried over to mouse xenotransplantation experiments, in which direct 2-HG treatment or introduction of IDH mutations led to decreased leukemic engraftment and an abrogated disease phenotypes. While the observed effects held true in a majority of the cell lines studies, Su *et al.* also identified several cell lines that were resistant to growth inhibition by 2-HG. By comparing 2-HG-resistant and –susceptible cell lines, they identified FTO as the only significantly differentially expressed α-KG dependent dioxygenase in susceptible cell lines. They further demonstrated that FTO is a target of 2-HG in both *in vitro* and cellular assays, and that 2-HG treatment increases m^6A content in resistant cell lines. In contrast, only 2-HG-resistant cell lines showed accumulation of 5hmC mediated by Tet2. Ultimately, they find that Myc, cell cycle (G2M), and E2F signaling pathways were downregulated upon 2-HG treatment in the susceptible cell lines, and that these changes were m^6A-dependent[75]. Of note, despite emerging evidence indicating that the true substrate of FTO is m^6A_m in the 5'UTR rather than m^6A, these authors maintain that loss of FTO in AML cell lines predominantly resulted in enhanced m^6A in gene bodies.

These findings suggest a significant revision of our understanding of IDH1/2 mutations, as they imply that IDH1/2 mutations intrinsically inhibit growth and proliferation of leukemia. Though the authors comment that these mutations may still have a role to play in early leukemic transformation, the proposed dissociation in function between disease initiation and maintenance is unexplained. The classification of 2-HG-resistant and -susceptible leukemic cell lines with distinct 2-HG-dependent effects is

another novel concept. The extent to which these findings in cell lines translate clinically is debatable. It is unclear, for example, if individual patients have exclusively FTO- or Tet2-dependent IDH1/2 mutant phenotypes, and whether this classification would correspond to diverging clinical outcomes.

As the authors note, IDH1/2 mutations lead to relatively favorable outcomes in glioma, and some evidence indicates that the same may be true in leukemia. However, this phenomenon has been largely attributed to differential sensitivity to existing therapeutics, rather than intrinsic disease-abrogating effects of 2-HG. For instance, several groups have reported impaired DNA damage responses in IDH mutant cells, which render them susceptible to traditional chemotherapeutics and radiation[25,76,77]. Clinical trial results with small molecule inhibitors of IDH1/2 also indicate that inhibition of 2-HG is an independently viable therapeutic modality, as enasidenib produces differentiation of myeloid cells and clinical benefits in refractory AML[78,79]. Ultimately, it would be informative to replicate the experiments discussed above in IDH1/2 patient samples to determine if the proposed model from cell line observations is replicated in clinical practice.

Hypothesis & Specific Aims

Hypothesis:

To date, many groups have published studies examining the effects of m^6A RNA modification in human and murine leukemia cell lines. Several of these studies have suggested differential effects of m^6A depletion on leukemic cells as compared to normal hematopoietic tissues. Our preliminary data suggest this is unlikely to be the case.

Rather, we hypothesize that the m^6A RNA modification regulates self-renewal and differentiation of hematopoietic stem cells, with corresponding effects on native hematopoiesis. Specifically we hypothesize that alterations in m^6A levels mediated by deletion of the methyltransferase METTL3 and the m^6A demethylase ALKBH5 will alter the frequencies of hematopoietic stem cells in the bone marrow of knockout mice, result in skewed hematopoietic differentiation. The observed phenotypes may have corresponding roles in myeloid malignancy, as has been reported elsewhere.

Aim 1: ***Phenotypic Characterization of METTL3 & ALKBH5 Knockout in Normal Hematopoiesis***

We will seek to characterize the effect of METTL3 and ALKBH5 deletion in native hematopoiesis by creating conditional knockout mice. Of note, mice with floxed METTL3 and ALKBH5 alleles allowing for Cre-mediated excision have recently been generated in the laboratory of Dr. Richard Flavell at Yale, which recently published effect of METTL3 knockout in CD4+ T cells[56]. These mice provide a powerful model system for the study of the m6A RNA modification in mammalian cells, and have been made available to us through collaboration with Huabing Li, of the Flavell lab, for characterization in the hematopoietic system.

Cre-Lox genome editing systems rely on the recognition of short 34 nucleotide LoxP sites flanking a large genomic targets. The Cre recombinase specifically recognizes a pair of LoxP sites, and mediates excision of the "floxed" intervening DNA sequence, allowing efficient gene deletion. Tissue-specific deletion of target genes can be accomplished by expressing the Cre recombinase downstream of a tissue-specific promoter.

To accomplish tissue-specific deletion of METTL3 and ALKBH5, we crossed METTL3$^{fl/fl}$ and ALKBH5$^{fl/fl}$ mice to mice expressing Cre under the control of the Vav promoter, generating Vav-Cre METTL3$^{fl/fl}$ mice, herein referred to as VCM3 mice. Vav is constitutively expressed in all hematopoietic tissues, with expression beginning during early embryonic hematopoiesis at day 10.5. Importantly, Vav affects HSC homeostasis without affecting the endothelial-to-hematopoietic transition (EHT) in the AGM[80,81]. This allows for isolation of an HSC- intrinsic phenotype, independent of the previously reported effects of METTL3 deletion on EHT[72]. Global knockout of METTL3 is known to be embryonic lethal, and we anticipated that constitutive METTL3 deletion in the hematopoietic compartment in Vav-Cre^{+}METTL3$^{fl/fl}$ mice would also result in non-viable embryos. With this in mind, we planned to use VCM3 mice to specifically address the role of METTL3 in fetal hematopoiesis by harvesting fetal liver at embryonic day 14.5 (E14.5). The fetal liver is an early site of embryonic hematopoiesis, and represents a transit site of hematopoietic stem cells following their emergence in the AGM, and prior to their final settlement in the adult bone marrow.

To assess the role of METTL3 in adult murine hematopoiesis, we will take advantage of inducible deletion mediated by expression of Cre under the control of the

Mx1 promoter in Mx1-Cre METTL3$^{fl/fl}$ mice, herein referred to as MCM3 mice. Mx1 is an interferon responsive-promoter, whose expression can is induced specifically in hematopoietic tissues and bone marrow stroma in response to treatment with poly-inosine-poly-cytodilic acid. This allows for time-specific, tissue-specific deletion of METTL3 in the hematopoietic compartment in adult mice[81]. Results from the analyses of these mice are forthcoming, and preliminary findings are discussed below.

Mice with global knockout of ALKBH5 have been derived previously and are known to be viable, though no specific analysis of the hematopoietic compartment has been published to date. We have similarly derived Vav-Cre ALKBH5$^{fl/fl}$ mice, herein referred to as VCA5 mice, for characterization.

We plan to characterize the hematopoietic phenotype of these mice by performing traditional assays of hematopoietic stem cell function. Specifically, we plan to perform: 1) Flow cytometry of fetal liver collected from embryos in the case of VCM3 mice, or peripheral blood, spleen and bone marrow collected from adult MCM3 and VCA5 mice. This will allow us to assess for the relative frequencies of immature hematopoietic stem and progenitor cells (HSPCs), as well as the composition of mature myeloid, erythroid, or lymphoid lineages; 2) Competitive transplant assays: In these assays an equal number of mutant and wildtype total bone marrow cells are transplanted into a lethally irradiated recipient mouse, and the relative contribution of each population is tracked over time. This allows for direct assessment of the relative fitness of knockout HSPCs compared to wildtype; 3) Colony forming unit (CFU) assays: Formation of hematopoietic colonies in semi-solid culture is a defining feature of HSCs. These assays provide an assessment of the ability of these cells to differentiate into lineage-specific

precursors including erythroid, myeloid, granulocyte-macrophage and megakaryocytic colonies; 4) Stress hematopoiesis assays: To assess for subtler effects in the context of external stressors, we will assess the response of wildtype and knockout mice to specific stressors including treatment with the chemotherapeutic agent 5-FU, as well as serial phlebotomy.

Aim 2: ***Molecular Characterization of VCM3, MCM3 and VCA5 mice***

To correlate the observed phenotypes of VCM3, MCM3, and VCA5 mice to molecular events driven by m^6A RNA modification, we will take advantage of fluorescence activated cell sorting (FACS) to prospectively identify specific subsets of hematopoietic cells of interest. Hematopoietic stem and progenitor cells (HSPCs) can be broadly identified by the exclusion of mature cells expressing lineage markers, in combination with the presence of the cell-surface markers Sca and cKit. This strategy identifies $Lin^-Sca^+c\text{-}Kit^+$ (LSK) cells, which broadly capture the HSPC compartment. The LSK fraction can be further stratified based on expression of the Slam family markers, which allow for the identification of long-term HSCs (LT-HSCs), short-term HSCs (ST-HSCs), multipotent progenitor (MPP), and more committed hematopoietic progenitor (HPC-1 & -2) populations[82].

An ideal characterization of these knockout mice would involve a combination of RNA-sequencing, RNA-lifetime profiling experiments, miCLIP, and ribosomal profiling of wildtype- and knockout-derived LSK cells. Unfortunately, LSK cells are infrequent, representing 0.3-0.5% of the total marrow, with approximately 30,000 cells per mouse, and no techniques exist for meaningful expansion of murine HPSCs in culture. While RNA-sequencing and half-life determinations should be feasible owing to the relatively

small cell numbers require for RNA-seq, both miCLIP and ribosomal profiling require 5-20ug of RNA, corresponding to approximately 30-50x10^6 cells[33]. This makes m6A profiling using primary murine tissues technically impossible.

To circumvent this issue, we will make use of the ER-HOXB8 cell line, which can be derived from murine hematopoietic progenitors. These cells express the oncogene HOXB8 under the control of the estrogen receptor. While maintained in estradiol-containing media, HOXB8 expression is enforced and these cells remain immortalized as myeloid precursors. Withdrawal of estradiol from the culture medium induces differentiation along the neutrophil lineage, and the extent of differentiation can be monitored by flow cytometry for the myeloid cell surface markers Gr1 and Mac1[83,84]. This provides an ideal model system for the study of myeloid differentiation, and would provide unlimited cell numbers for miCLIP & Ribo-Seq characterization.

An alternative approach would be to perform miCLIP and Ribo-Seq on less stringent subsets of hematopoietic cells. One reasonable option would be to isolate Lin^- c-Kit^+ (LK) cells, which represent a larger overall fraction of the cells, while still enriching for HSPCs, which are uniformly c-Kit^+. The obvious limitation to this approach is that it provides a less pure signal. Nevertheless, a similar approach has been used in the study of m6A in early hematopoiesis in zebrafish, in which the entire trunk region including the AGM was homogenized and sequenced. The data produced should ultimately be reflective of the m^6A profile of hematopoietic precursors, and should rely the identification of some – but not necessarily all – relevant targets.

Lastly, in addition to traditional bulk RNA-seq of LSK cells, we propose single cell RNA-sequencing (scRNA-seq) of LSK cells isolated from wildtype and knockout

mice. Where RNA-sequencing provides information about bulk changes in overall gene expression, scRNA-seq provides phenotype information, as cell identity can be inferred from transcriptional profile[85]. This would therefore allow for the identification of relatively more or less immature HSCs within the LSK fraction, while simultaneously identifying the transcripts underlying the observed changes.

Methods

Statement of Research

I independently developed the hypothesis and initial experimental design for this work. I independently designed and performed the HOXB8 cell line experiments. Design of the VCM3 experiments was further developed with Dr. Halene & Yimeng Gao. The data in Figure 5 were independently collected and prepared by Yimeng Gao & Yuanbing Song. The experiments presented in Figures 6-9 were performed by Yimeng Gao & I, and the data were analyzed by Yimeng Gao. The VCA5 experiments presented in Figures 10-13 were performed by Yimeng Gao & I, and I analyzed the data. I independently performed the experiments and analyzed the data for Figures 14 & 15. Bioinformatic analyses of RNA-seq data for Figure 16 & 17 were performed by Toma Tobaldi

Statistics

All data presented were compared using unpaired two-tailed student's t-test. Statistical significance indicated on graphs as follows: * $p<0.05$, ** $p<0.01$, *** $p<0.001$, **** $p<0.001$. Data are presented with mean +/- S.E.M.

HOXB8 Cell Line Assays

HOXB8 cell lines were a gift of David B. Sykes and Peter Gaines, and were named the DBS and PG cell lines, respectively. The DBS cell lines were derived from a mouse expressing a GFP reporter downstream of the myeloid lineage gene Lysozyme. PG cell lines were derived from a wildtype mouse with no fluorescent reporter. HOXB8 cells were cultured in OPTI-MEM with 10% heat-inactivated certified FBS, 2mm L-Glutamine, 5U/mL pencillin G, 5ug/mL streptomycin sulfate with 2% SCF-conditioned mediated derived from CHO-SCF producer cell lines, with 0.5uM β-Estradiol.

Differentiation media was identical, with the exception of β-Estradiol, which was not used. We used anti-CD11b Pacific Blue and anti-Gr1 APC antibodies for flow cytometric assessment at 24, 48, 72, and 96h following β-Estradiol withdrawal.

Puromycin-selectable shRNAs targeted against METTL3 (TRCN0000039111, TRCN0000039112, TRCN0000039113) and FTO (TRCN0000183897, TRCN0000277143) were purchased from Sigma-Mission. These were assembled into Lentivirus by transfecting 293FT cells with a pCMV-VSV-G envelope vector, psPax2 2nd generation packaging vector, and the shRNA plasmid. Viral supernatants were collected every 24 hours for four days and purified using Millipore Centrifugal Filter Units (100K). HOXB8 cells were trasduced with lentivirus by plating 1x10^{6} HOXB8 cells in 500 µL media in a 24 well plate with 8µg/µL polybrene, and 10µL virus. After 8 hours, 500µL fresh media was added, and after 24 hours, transduced cells were transferred into 6 well plates with 4mL additional media, with 3µg/µL puromycin.

METTL3 & VCA5 Mice

METTL3 & ALKBH5 conditional knockout mice were a kind gift of Hua-Bing Li of the Flavell lab, generated as previously described[56].

Mouse Sacrifice & Sample Collection

VCA5 & VCM3 mice were sacrificed in accordance with existing IACUC guidelines and protocols. Mice were anesthetized with inhaled 30% Isofluorane, and peripheral blood samples were collected by retro-orbital bleeding. Sacrifice was then performed by cervical dislocation. Bone marrow samples were collected from femurs and tibia, with each bone flushed 3x with 1mL FACS buffer (PBS + 0.5% BSA + 2uM

EDTA). Spleen & thymus were harvested, mechanically dissociated in FACS buffer, and passed through a 40μm cell strainer (Falcon).

Flow Cytometry Assessment of Fetal Liver & Bone Marrow Populations

Flow cytometry experiments were performed on a BD FACSARIAII. Red blood cell lysis was performed as necessary using ACK Red Blood Cell Lysis Buffer (Thermo Fisher). Samples were treated with purified rat anti-mouse CD16/32 (BD Biosciences) to block the Fc receptor as necessary. Samples were then stained with the appropriate antibody panels. Antibodies used include: anti-CD41 FITC (Pharminogen), anti-CD48 Pac Blue (BioLegend), anti-CD150 PeCy5 (BioLegend), andti-CD105 PeCy7 (BioLegend), anti-cKit APC (BioLegend), Lineage Biotion (BD Bioscience), Streptavidin APC-Cy7 (BioLengend), anti-Gr1 Biotin (BioLegend), anti-B220 Biotion (BioLegend), anti-CD11b Biotin (BioLegend), Streptavidin eFluor 450 (eBioSciences), anti-Ter119 (eBioSciences), anti-CD44 APC (BioLegend), anti-CD71 PECy7 (BioLegend), anti-CD34 FITC (eBioSciences), anti-CD16/32 (eBioSciences), anti-Gr1 APC (eBioSciences), anti-CD11b Pac Blue (eBioSciences), anti-CD3 FITC (BioLegend), anti-B220 APC-Cy7 (BioLegend), anti-CD45.1 PECy7 (Biolegend), anti-CD45.2 PE (Biolegend), anti-7/4 PE (Biolegend), anti-CD4 APC Cy7 (BioLegend), anti-CD8a Biotin (Pharminigen), anti-CD25 PE (BioLegend), CD44 PE-Cy5 (eBioSciences).

Colony Forming Assays

10,000 fetal liver or bone marrow cells were mixed in 3mL of MethoCult GF M3434 for mouse cells (StemCell Technologies) and plated in triplicate. Plates were incubated for 12-14 days at 37^{o}C in 5% CO2, and then morphologically evaluated and counted.

VCM3 Transplant Assays

Hematopoietic reconstitution assays with VCM3 mice were performed engrafting lethally-irradiated congenic CD45.1 Pep3/B 4-6 week-old recipient mice with $1x10^6$ CD45.2 VCM3 WT or KO fetal liver cells. Competitive transplant was performed with VCM3 mice by mixing $0.5x10^6$ CD45.2+ VCM3 WT or KO fetal liver cells with an equal number of CD45.1+ competitor bone marrow cells and injected mixtures into lethally irradiated CD45.1/2 double positive recipient mice. Recipient mice in each group were matched for age & gender. Peripheral blood and bone marrow engraftment were assessed at 8 days post-transplant, consistent with the observed timeline of VCM3 KO mortality in hematopoietic reconstitution assays.

VCA5 Competitive Transplant Assays

CD45.1/2 double-positive recipient mice were lethally irradiated (850 cGy) and engrafted with $0.5x10^6$ CD45.2 VCA5 WT or KO total bone marrow cells, and an equal number of competitor CD45.1 Pep3/B total bone marrow cells. Peripheral blood chimerism was assessed every two weeks, starting at 4 weeks post-transplant.

RNA Extraction & qPCR

RNA extraction was performed with the Qiagen RNeasy Mini Kit, and SYBR Green was used for qPCR quantification of transcript abundance (Thermo-Fisher).

RNA Sequencing

RNA-seq experiments were performed in biological triplicate on Illumina HiSeq 2500. All programs were used with default settings. Raw reads were processed with Trimmomatic (v0.36) and aligned to the mouse genome (GRCm38) with STAR (v2.5.3a --quantMode GeneCounts), using the Gencode M15 transcript annotation as a

transcriptome guide. Normalization and differential analysis between Mettl3 WT and KO gene expression levels were performed with the edgeR Bioconductor package. Differentially expressed genes were identified with the following thresholds: 1) mean normalized counts per million > 1, 2) absolute log2 Fold Change > 0.75, 3) False Discovery Rate (FDR) < 0.05.

Functional annotation of gene lists and enrichment analysis with Gene Ontology terms and Enrichr gene-set libraries (http://amp.pharm.mssm.edu/Enrichr/) were performed with the clusterProfiler and enrichR R packages. Enrichment with False Discovery Rate (FDR) < 0.05 were considered statistically significant.

Results

METTL3 Knockdown Results in Delayed Differentiation of ER-HOXB8 Cells

To determine if the m^{6}A machinery has a role in normal myelopoiesis, I performed shRNA knockdown of m^{6}A writer & eraser proteins in the ER-HOXB8 immortalized murine myeloid progenitor cell line. These cells express the oncogene HOXB8 under the control of the estrogen receptor. While maintained in estradiol-containing media, HOXB8 expression is enforced and these cells remain as immature myeloid precursors. Withdrawal of estradiol from the culture media induces differentiation along the neutrophil lineage, and the extent of differentiation can be monitored by flow cytometry for the myeloid cell surface markers Gr1 and Mac1[83,84]. With differentiation, these cells proceed from *Gr1$^-$Mac1$^-$* to *Gr1$^+$Mac1$^+$* (Fig. 1).

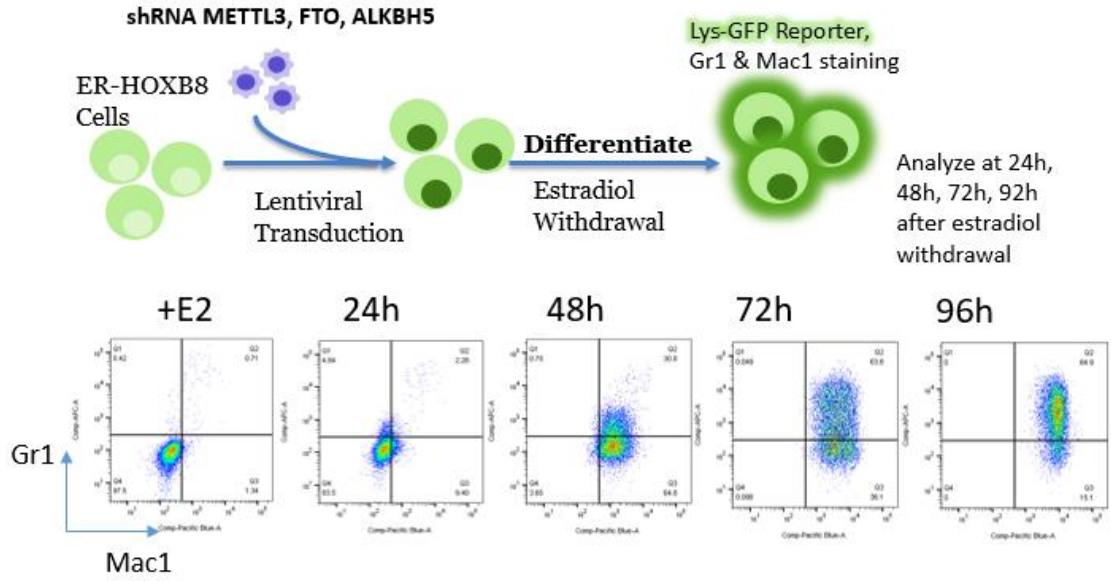

Figure 1: ***Experiment schematic with representative differentiation time course***. ER-HOXB8 cells underwent lentiviral transduction with shRNA targeted against FTO, METTL3, & ALKBH5, and puromycin selection. Following Estradiol withdrawal, ER-HOXB8 cells were allowed to differentiate, with flow cytometry for CD11b, Gr1, and GFP performed every 24 hours. Flow cytometry plots show a representative differentiation time course. Differentiation time course adapted from *Sykes et al., 2016.*

I performed shRNA-mediated knockdown of METTL3 and FTO in two independently-derived ER-HOXB8 cell lines, labeled “DBS” and “PG”. The DBS cell line was derived from the marrow of mice expressing a GFP reporter under the control of the Lysozyme promoter, which serves as a surrogate indication of myeloid differentiation. The PG cell line was derived from wildtype murine marrow. Lentivirus was produced using shRNA plasmid purchased from Sigma, and cells were spinfected (Fig. 1). Knockdown efficiency was determined by qPCR. METTL3 knockdown of ~40-70% was accomplished with three separate shRNAs (sh111, sh112, sh113) compared to control shRNA (shCOO2) and the untransduced (WT) parental cell line. FTO knockdown efficiency was ~50-55% (sh183), and ~75-80% (sh227) (Fig. 2). While I similarly attempted to derive ALKBH5 knockdown cell lines, these were variable in knockdown efficiency, and knockdown efficiency was frequently lost during culture and in vitro differentiation.

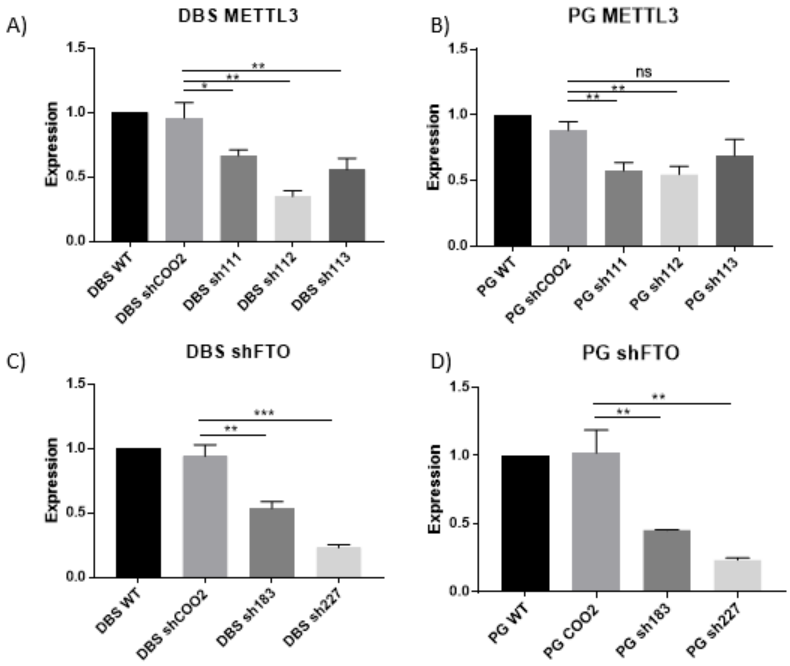

Figure 2: ***METTL3 knockdown efficiency by qPCR*** in A) DBS HOXB8 cells, B) PG HOXB8 cells; and FTO knockdown efficiency in C) DBS HOXB8 cells & D) PG HOXB8 cells (n=3 replicates for all groups).

Surprisingly, METTL3 knockdown resulted in delayed differentiation, as reflected by delayed acquisition of the myeloid markers CD11b and Gr1 (Fig. 3). This was consistent in both independently-derived cell lines. This effect was also uniform across all shRNAs targeted against METTL3. Data from 72h for the DBS cell line (Fig. 3A) and 96h for the PG cell line (Fig. 3B) are shown as these were the most directly comparable time points, but the same trends were observed at 72h in the PG cell line. These results suggest that loss of METTL3 impairs myeloid differentiation in this *in vitro* model.

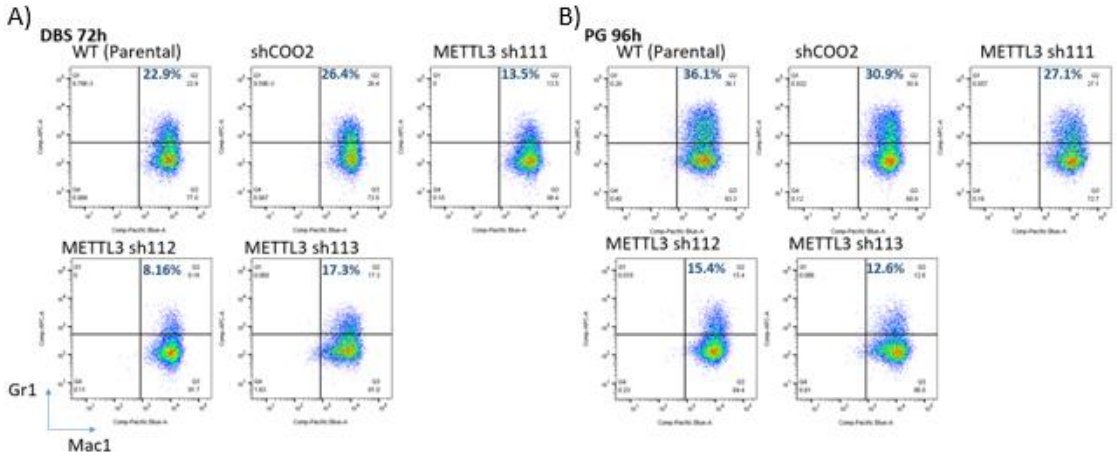

Figure 3*: **Flow cytometry for myeloid differentiation markers CD11b (Mac1) & Gr1 in METTL3 knockdown cell lines.*** A) DBS ER-HOXB8 cells at 72h after estradiol withdrawal and B) PG ER-HOXB8 cells at 96h after estradiol withdrawal. Data are shown for Parental (untransduced) cells, control shRNA (shCOO2) and three different shRNAs.

Knockdown of FTO yielded less consistent results. While knockdown of FTO with sh227 did result in a striking delay in differentiation in both DBS & PG cells, knockdown with sh183 did not show any notable changes from untransduced cells or those transduced with control shRNA (Fig. 4). These results could be clarified further by repeating this experiment with additional shRNAs targeted against FTO, or by CRISPR mediated deletion of FTO.

Importantly, these results are the product of a single pilot experiment which was not repeated. The consistent METTL3 knockdown phenotype across independently-derived ER-HOXB8 cells lines and multiple shRNAs is striking. Nevertheless, these findings are not definitive. This would require replication of the results, and verification that the observed phenotypes are m^6A-mediated by m^6A quantification techniques and demonstration that the effect is reversed by rescue of METTL3 expression. These preliminary data did, however, provide an indication of a likely hematopoietic phenotype and prompted further investigation.

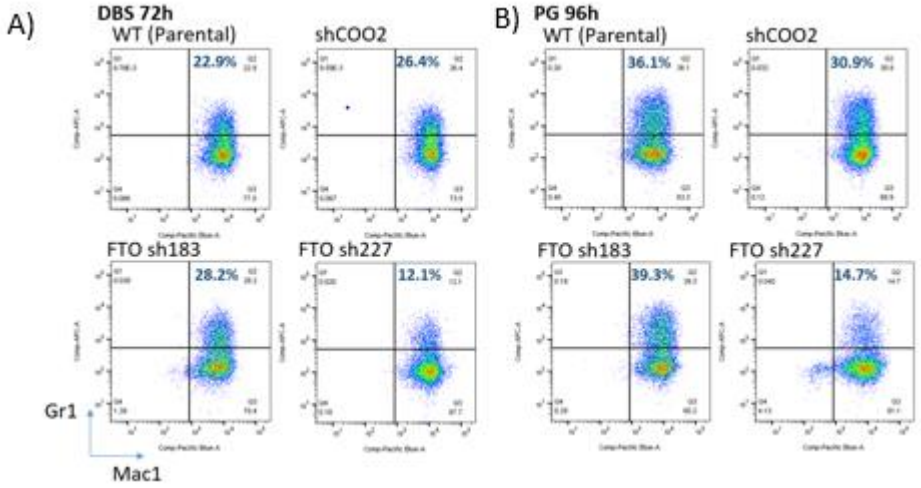

Figure 4: ***Flow cytometry for myeloid differentiation markers CD11b (Mac1) & Gr1 in FTO knockdown cell lines*** A) DBS ER-HOXB8 cells at 72h after estradiol withdrawal and B) PG ER-HOXB8 cells at 96h after estradiol withdrawal. Data are shown for Parental (untransduced) cells, control shRNA (shCOO2) and two different shRNAs.

METTL3 is Essential for Murine Hematopoiesis

Having briefly examined a role for m^6A in an *in vitro* model, we proceeded to characterize the hematopoietic phenotypes of VCM3 mice. I will refer to Vav-Cre^+ $METTL3^{fl/fl}$ mice as VCM3 KO, Vav-Cre^+ $METTL3^{+/fl}$ as VCM3 HET and VCM3 WT will refer to either Vav-Cre^+ $METTL3^{+/+}$ or Vav-Cre^- $METTL3^{fl/fl}$.

Loss of METTL3 in the hematopoietic compartment of VCM3 KO mice was uniformly fatal. The yield of VCM3 mice from defined breeding pairs (Fig. 5A) deviated significantly from the expected Mendelian ratios (Fig. 5B, Table 1). Of the few VCM3 KO pups that were born, all died shortly after birth. VCM3 KO pups demonstrated marked pallor and decreased size compared to HET or WT littermates (Fig. 5C). Given the apparent embryonic lethality of VCM3 KO mice, we analyzed fetal liver at embryonic day 14.5 (E 14.5). At this time-point, definitive hematopoiesis has emerged, and the fetal liver serves as the primary hematopoietic organ prior to migration of the hematopoietic system to the mature bone marrow. Of note, expression of Vav begins in primitive hematopoietic tissues at E11.5, allowing for Cre-mediated excision of METTL3 after definitive HSC emergence[80,86]. Mendelian ratios at E14.5 were as expected (Fig. 5B). Loss of METTL3 was confirmed in KO fetal liver by qPCR, while HET mice maintained expression similar to WT (Fig. 5D). VCM KO fetal liver exhibited decreased total cellularity compared to HET or WT (Fig 5E), and expression of key hematopoietic transcription factors Myb, Pu.1 and Rag1 were disturbed (Fig. 5F). Myb & Rag1 were increased in expression, while Pu.1 was downregulated. Of note Myb has been implicated as a target of m^6A, while Pu.1 is believed to regulate the function of METTL14[40]. To date, Rag1 has not been previously implicated as an m^6A-modified transcript.

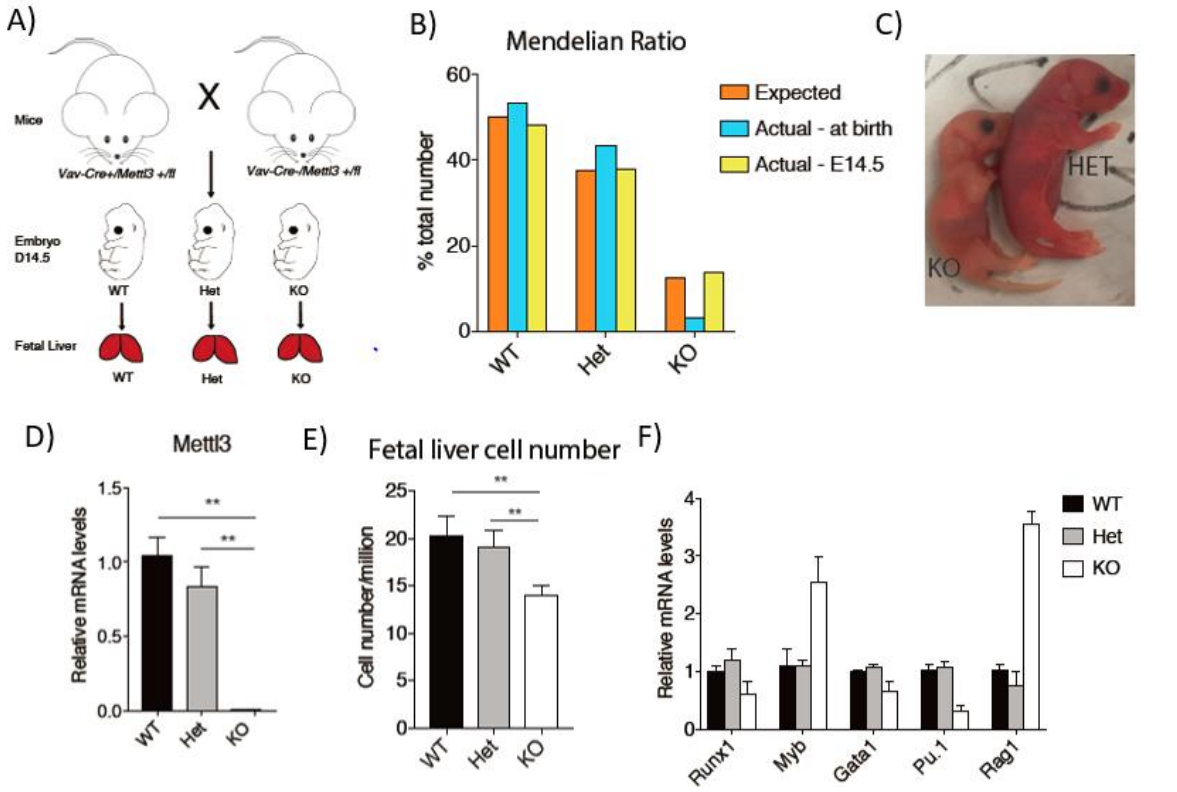

Figure 5*: **Initial characterization of VCM3 mice***. A) Breeding & experimental schematic B) Expected Mendelian ratios based on breeding schematic plotted against observed genotype ratios at birth and at time of fetal liver harvest at E 14.5. C) Appearance of VCM3 HET & VCM3 KO mice. D) METTL3 expression by qPCR on fetal liver hematopoietic tissue (n=3 replicates per group) E) Fetal liver cellularity of VCM3 mice (n=3 per group) F) Expression of hematopoietic transcription factors by qPCR on fetal liver from VCM3 mice. (n=3 replicates per group).

Table 1. Mendelian Ratio of Vav-Cre Mettl3 mice

Genotype	WT	Het	KO
Expected Ratio	50.0% (4/8)	37.5% (3/8)	12.5% (1/8)
Actual Birth Ratio	53.30%	43.30%	3.30%(dead)
Actual Fetal Liver Ratio	48.30%	37.90%	13.80%

Table 1*: **Expected & observed Mendelian ratios.*** Mendelian ratios based on breeding schematic compared with observed ratios at birth, and at time of fetal liver analysis at E 14.5.

These findings indicate that METTL3 is essential for murine hematopoiesis, and that loss of METTL3 within the hematopoietic compartment is embryonic lethal. Based on the normal yield of VCM3 KO mice consistent with the expected Mendelian ratios at E14.5, lethality occurs at some point after the emergence of hematopoiesis at E14.5 (Fig. 5C). The observed disturbances in cell number and gene expression do, however, indicate dysfunction at this early time-point.

Altered Frequency & Function of HSPCs in VCM3 Fetal Liver

To assess the effects of METTL3 deletion on HSPCs, we assessed the frequency of distinct HSPC populations by flow cytometry. We first assessed the frequency of Lin^- $c\text{-}Kit^+$ and LSK populations in VCM3 mice (Fig. 6A). VCM3 KO mice exhibited a significantly increased proportion of LSK cells, while the frequency of $Lin^-c\text{-}Kit^+$ cells was identical (Fig. 6B). There was a trend towards an increase in the Lin^- fraction in KO cells that did not achieve statistical significance (Fig. B; WT vs KO: p=0.0503, HET vs KO: p=0.0975) due to small sample size (n=2 per group). Further examination of the LSK compartment showed increased frequencies of HPC-1 progenitor cells ($CD150^-$ $CD48^+$), which are predominantly lymphoid restricted progenitors, in VCM3 KO fetal liver (Fig. 6C, D). There was also a trend towards increased HPC-2 ($CD150^+CD48^+$). To assess the ability of VCM3 fetal liver HSPCs to contribute to definitive hematopoiesis, we performed colony forming unit (CFU) assays. CFUs provide a quantitative surrogate measure of the ability of HSPCs to differentiate along specific lineages. For these assays 10^5 total fetal liver cells were plated in methylcellulose supplemented with hematopoietic growth factors in triplicate. Colonies were morphologically evaluated and counted 12-14 days after plating. VCM KO fetal liver HSPCs gave rise to a significantly lower number

of total colonies, with a significant reduction of BFU-E (burst-forming unit – erythroid) and CFU-GEMM (granulocyte, erythroid, megakaryocyte, monocyte) (Fig. 6E). These results suggest impaired hematopoietic function despite the presence of an increased proportions of LSK HPSCs.

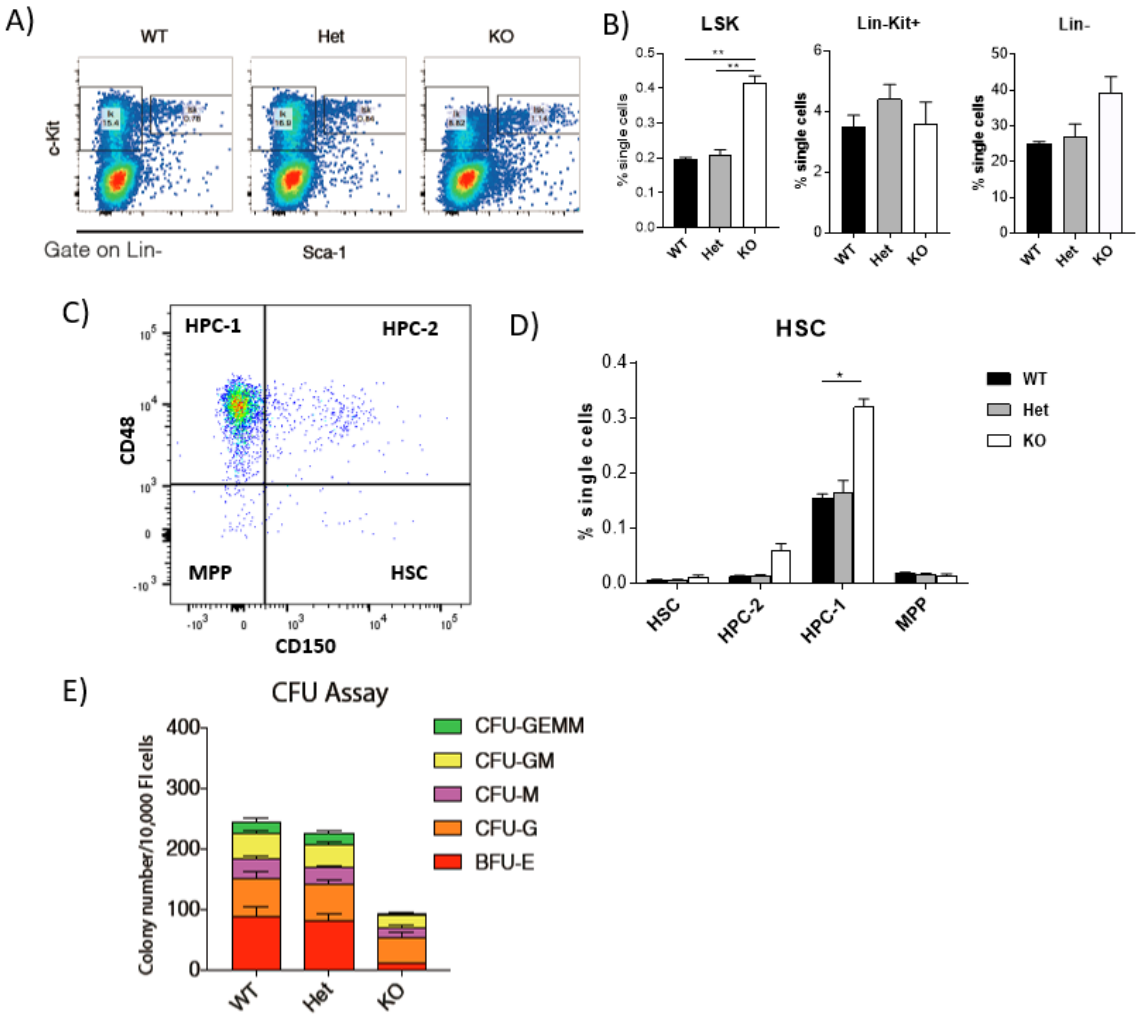

Figure 6: ***Characterization of the HSC compartment in VCM3 mice***. A) Gating of Lin-Kit+ and LSK populations in VCM3 WT, HET & KO mice. B) Frequency of LSK, Lin-Kit+ and Lin- cells in VCM3 mice, plotted as percentage of total marrow cellularity (n=2 per group) C) Subgating of LSK population into Hematopoietic Stem Cell (HSC), Hematopoietic Progenitor Cell-1 & -2 (HPC-1, HPC-2) and Multipotent Progenitors (MPP) D) Frequency of HSC, HPC-1, HPC-2 and MPP populations as percentage of total marrow cellularity (n=2 per group). E) Colony Forming Unit (CFU) Assay. ***CFU-GEMM***: Colony Forming Unit Granulocyte-Erythrocyte-Macrophage-Megakaryocyte; ***CFU-GM*** Colony Forming Unit Granulocyte Macrophage; ***CFU-M***: Colony Forming Unit Macrophage; ***CFU-G***: Colony Forming Unit Granulocytes ***BFU-E***: Burst Forming Unit Erythroid (n=3 per group).

HSCs are functionally defined by their ability to serially reconstitute the full hematopoietic hierarchy in lethally irradiated recipient mice. Bone marrow transplantation assays therefore serve as the gold-standard assay of HSC self-renewal and differentiation. To determine if fetal-liver derived VCM3 HSPCs could reconstitute hematopoiesis, we engrafted lethally-irradiated congenic CD45.1 Pep3/B 4-6 week-old recipient mice with $1x10^6$ CD45.2 VCM3 WT or KO fetal liver cells. While VCM3 WT fetal liver rescued lethally irradiated recipients, all VCM3 KO fetal liver recipients died by day 14, at the time of expected hematopoietic recovery (Fig. 7A). Correspondingly, engraftment of CD45.2 VCM KO cells was drastically diminished in the bone marrow and peripheral blood of recipient mice compared to those receiving WT fetal liver (Fig. 7B-D).

To ensure that decreased engraftment and mortality in these mice was not a technical artefact, we mixed CD45.2+ VCM3 WT or KO fetal liver cells with an equal number of $CD45.1^+$ bone marrow cells and injected mixtures into lethally irradiated CD45.1/2 double positive recipient mice. This allows for tracking of the relative contributions of each competing donor population following transplantation. The degree of marrow chimerism is an indication of the relative fitness of HSPCs compared to the wildtype competitor marrow. Whereas VCM3 WT cells repopulated recipient mice in equal proportion with $CD45.1^+$ competitor cells, recipients receiving VCM3 KO marrow were almost entirely reconstituted by the $CD45.1^+$ cells at 6 weeks, with few persisting CD45.2 cells (data not shown) Cumulatively, these findings imply defective homing, self-renewal, or differentiation abilities of VCM3 KO HSPCs.

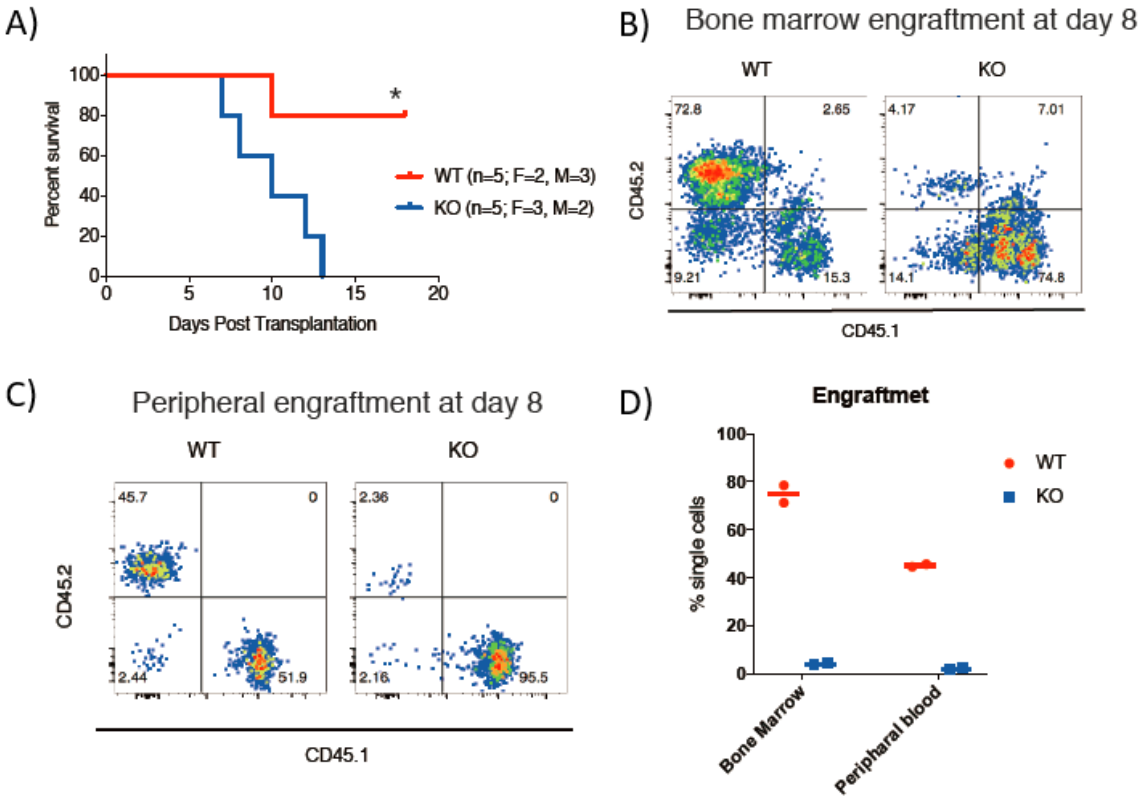

Figure 7: ***Transplantation assay using VCM3 bone marrow.*** A) Survival curves for VCM3 WT & KO mice. Mouse numbers and gender indicated on figure. B) Engraftment of CD45.2 VCM3 WT or KO cells in the bone marrow and C) Peripheral blood of CD45.1 recipient mice at 8 days post-transplant. D) Engraftment of CD45.2+ VCM3 donor cells in the bone marrow and peripheral blood (n=2 per group).

To determine if VCM KO fetal liver HSPCs exhibit homing defects, we labeled VCM3 fetal liver cells with the membrane dye CFSE and injected them into lethally-irradiated recipient mice. Recipients were euthanized 16 hours later, and engrafted donor cells were quantified by the combination of CD45.2 and CFSE (GFP) on flow cytometry. No differences in homing were detected, suggesting that VCM3 KO fetal liver HSPCs fail to reconstitute hematopoiesis due to loss of self-renewal or differentiation ability.

VCM3 Fetal Liver Exhibits Altered Erythropoiesis

As noted previously, VCM KO pups that survived until birth exhibited marked pallor, and CFU assays showed decreased propensity for the formation of erythroid colonies. To explicitly assess VCM3 fetal liver for defects in erythropoiesis, we assessed the distribution of erythropoietic precursors based on CD44 staining of Ter119+ cells. As erythrocytes develop, they gradually decrease in size and lose expression of CD44. As this process occurs these cells progress sequentially through defined stages starting with the immature proerythroblasts (I), followed by the basophilic erythroblast (II), polychromatic erythroblast (III), orthochromatic erythroblast (IV), reticulocyte (V) and mature red blood cell (VI) stages[87] (Fig. 8A).

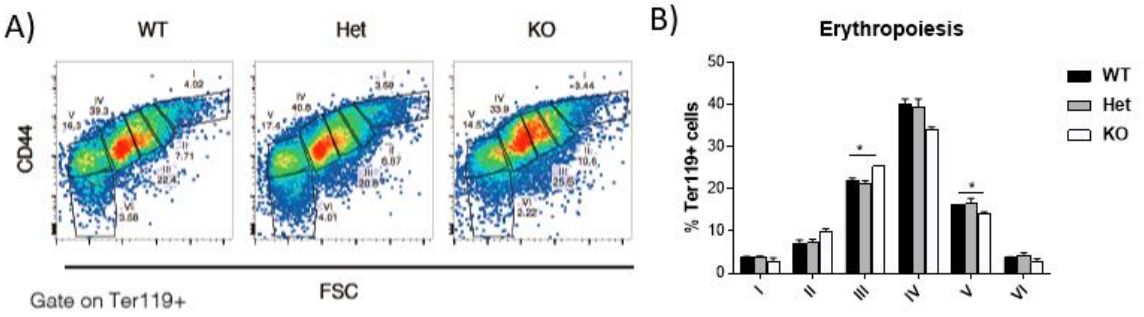

Figure 8: ***Erythropoiesis in VCM3 fetal liver.*** A) Gating of erythrocyte precursors based on CD44 staining progression demonstrating Proerythroblasts (I), Basophilic Erythroblasts (II), Polychromatic Erythroblasts (III), Orthochromatic Erythroblasts (IV), Reticulocytes (V) and mature Red Blood Cells (VI) in VCM3 fetal liver. B) Frequency of erythrocyte stages I-VI as percentage of Ter119+ fetal liver cells (n=2 per group).

Assessing this pattern of differentiation, we a found small but statistically significant increase in immature polychromatic erythroblasts (III), and a significant decrease in more mature reticulocytes (V). There were striking trends towards significant decreases in orthochromatic erythroblasts (IV) and reticulocytes (VI), but these failed to attain significance, again owing to low sample size (n=2) (Fig. 8B). These findings may be indicative of the early onset of an erythropoietic defect that may account for the

embryonic lethal phenotype, as well as the observed pallor of VCM3 KO mice that survived to birth.

Myeloid Progenitor Depletion and Enhanced Differentiation in VCM3 Fetal Liver

Several studies have noted that differentiation blockade in AML cell lines resolves in response to METTL3 knockdown or knockout based on increased CD11b expression [38,73]. Recently published evidence from inducible METTL14 knockout mice similarly suggests an increased leukocyte count, and enhanced myelopoiesis[40].

To explore the effect of METTL3 knockout on myeloid differentiation, we assessed the frequency of myeloid precursors and mature myeloid cells in VCM3 fetal liver. Myeloid progenitors including granulocyte-macrophage progenitors (GMP), common myeloid progenitors (CMP) and megakaryocyte erythroid progenitors (MEP) can be identified based on expression of FcRγ (CD16/32) and CD34 (Fig. 9A), while mature myeloid cells were quantified by expression of CD11b (Fig. 9C) and the activated neutrophil marker 7/4. These experiments showed a decreased number of GMP and CMP in VCM3 KO mice (Fig 9A,B), accompanied with a small, but significant increase in mature myeloid cells, from ~3.5% in WT or HET fetal liver to ~6.5% in KO liver (Fig 9C, D). There were few activated neutrophils overall, but there was a significant increase in $7/4^+$ neutrophils in VCM3 KO compared to WT & HET (Fig 9D).

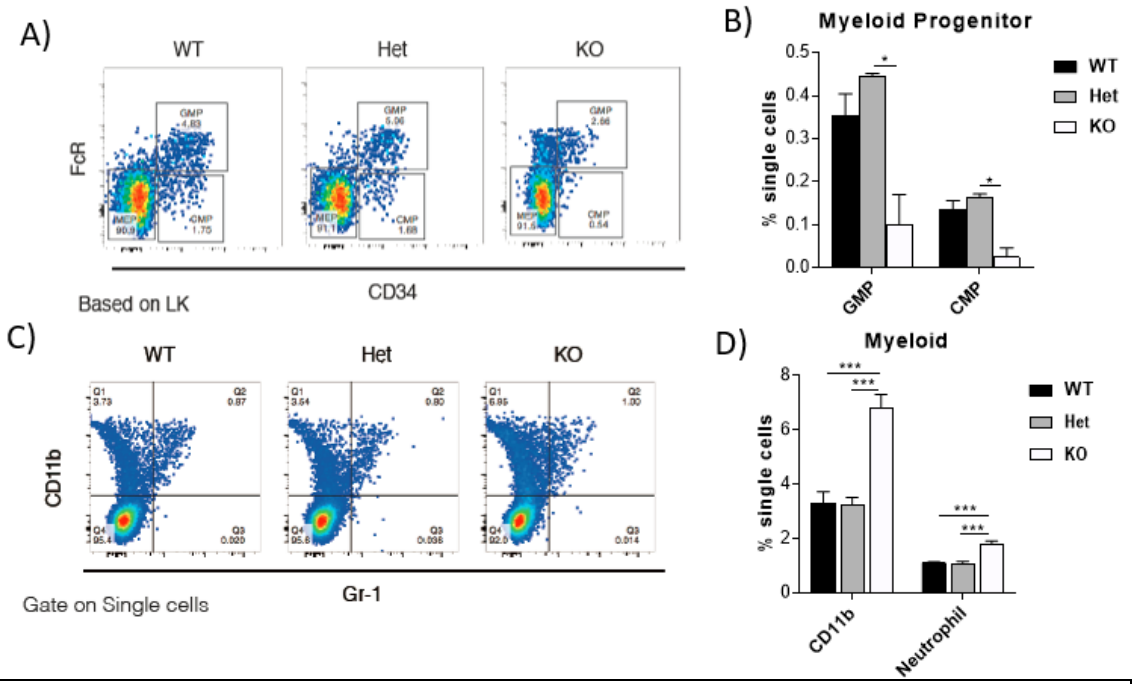

Figure 9: ***Myelopoiesis in VCM3 fetal liver.*** A) Representative data from VCM3 WT, HET & KO fetal liver illustrating gating scheme for myeloid progenitors including Common Myeloid Progenitor (CMP), Granulocyte-Macrophage Progenitor (GMP) & Megakaryocte-Erythroid Progenitor (MEP). B) Frequency of GMP & CMP in VCM3 fetal liver plotted as percentage of total fetal liver cellularity (n=2 mice per group). C) Representative data from VCM3 fetal liver illustrating gating scheme for mature myeloid cells based on CD11b and Gr1 staining of VCM3 fetal liver. D) Frequency of CD11b+ and activated neutrophils ($7/4^{+}$) as percentage of total fetal liver cellularity in VCM3 mice. (n=3 mice per group).

These findings indicate depletion of myeloid progenitors with an increase in mature myeloid cells in VCM3 KO fetal liver. These findings are consistent with the previously published results, though it should be noted that myelopoiesis is limited in the context of the fetal liver, as reflected by the low overall frequency of myeloid cells. The effects of METTL3 on myeloid development would be further clarified through inducible knockout of METTL3 in adult murine marrow, in which myeloid cells are much more abundant.

Normal Myelopoeisis, Lymphopoiesis, and Erythropoiesis in VCA5 Mice

Having identified a prominent role for METTL3 in hematopoiesis, we next sought to determine whether the m^6A demethylase ALKBH5 had corresponding effects. Of note, while knockout of METTL3 induces drastic, genome-wide reductions of m^6A, loss of ALKBH5 results in very subtle changes in net m^6A content of cellular RNA. Constitutive ALKBH5 knockout mice live normal lifespans, and their only reported phenotype thus far is altered spermatogenesis and decreased fertility[28].

In the following text, I will refer to Vav-Cre^+ $ALKBH5^{fl/fl}$ mice as VCA5 KO, Vav-Cre^+ $ALKBH5^{+/fl}$ as VCA5 HET and VCA5 WT will refer to either Vav-Cre^+ $ALKBH5^{+/+}$ or Vav-Cre^- $ALKBH5^{fl/fl}$.

To assess for hematopoietic phenotypes in the conditional VCA5 KO mice, we first evaluated the proportion of mature myeloid and lymphoid tissues in 4-6 week old mice. The frequency of myeloid cells was assessed by flow cytometry for CD11b and Gr1, while the B & T cell compartments were assessed by B220 and CD3 expression, respectively. In two independent experiments, analysis of the bone marrow, peripheral blood and spleen revealed no significant differences in myeloid or lymphoid cell frequency between VCA5 KO and WT mice (Fig. 10A, B).

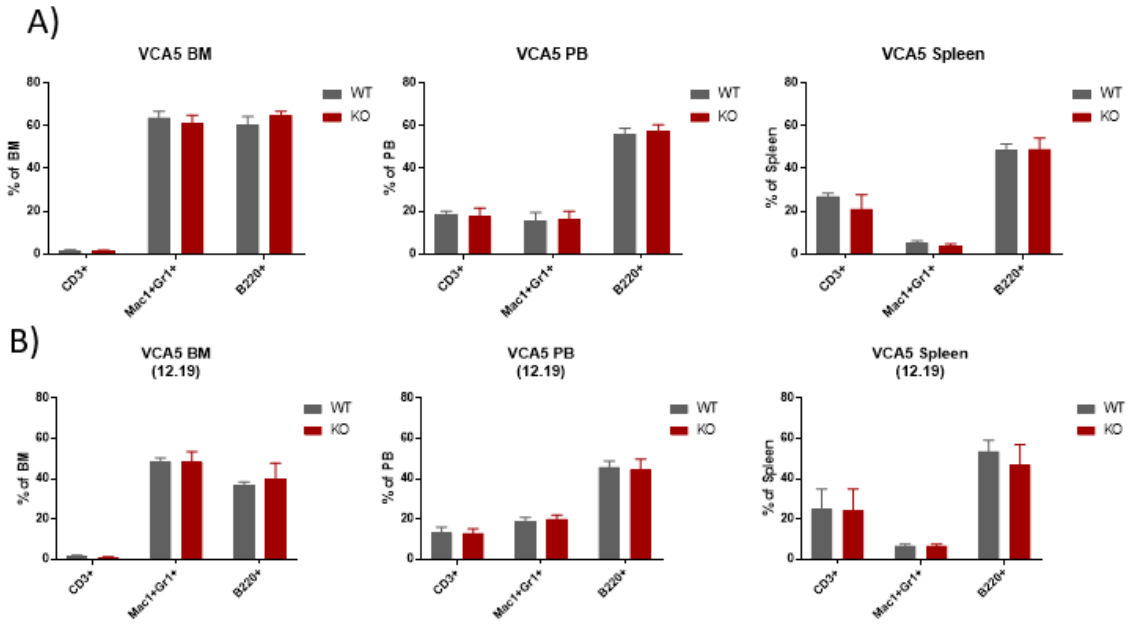

Figure 10: ***Marrow, Spleen & Peripheral Blood Characterization of VCA5 mice.***
A) & B) Frequency of CD3+ T Cells, B220+ B Cells and Mac1+Gr1+ myeloid cells in the bone marrow (BM), peripheral blood (PB), and spleen of 4-6 week old VCA5 WT & KO mice. The two panels represent the results of two independent experiments (n=3 per group).

A previously published study showed that loss of METTL3 in CD4+ T cells results in persistently naïve T cells. To assess the effect of ALKBH5 knockout on T cells, we harvested thymus from 4-6 week old mice[56]. Staining with CD44 and CD25 allows identifies immature double negative (DN) T cell stages (DN 1-4)[88,89]. CD4 marks T helper cells, CD8 identifies cytotoxic T cells, and uncommitted double positive (DP) T cells express both (Fig. 11A, B). We observed no significant differences in these T cell populations in the thymus. This is consistent with the original T cell data, as METTL3 KO mice had T cell phenotypes in the lymph nodes and spleen, but not in the thymus. We will need to analyze lymph node tissue for a more thorough characterization.

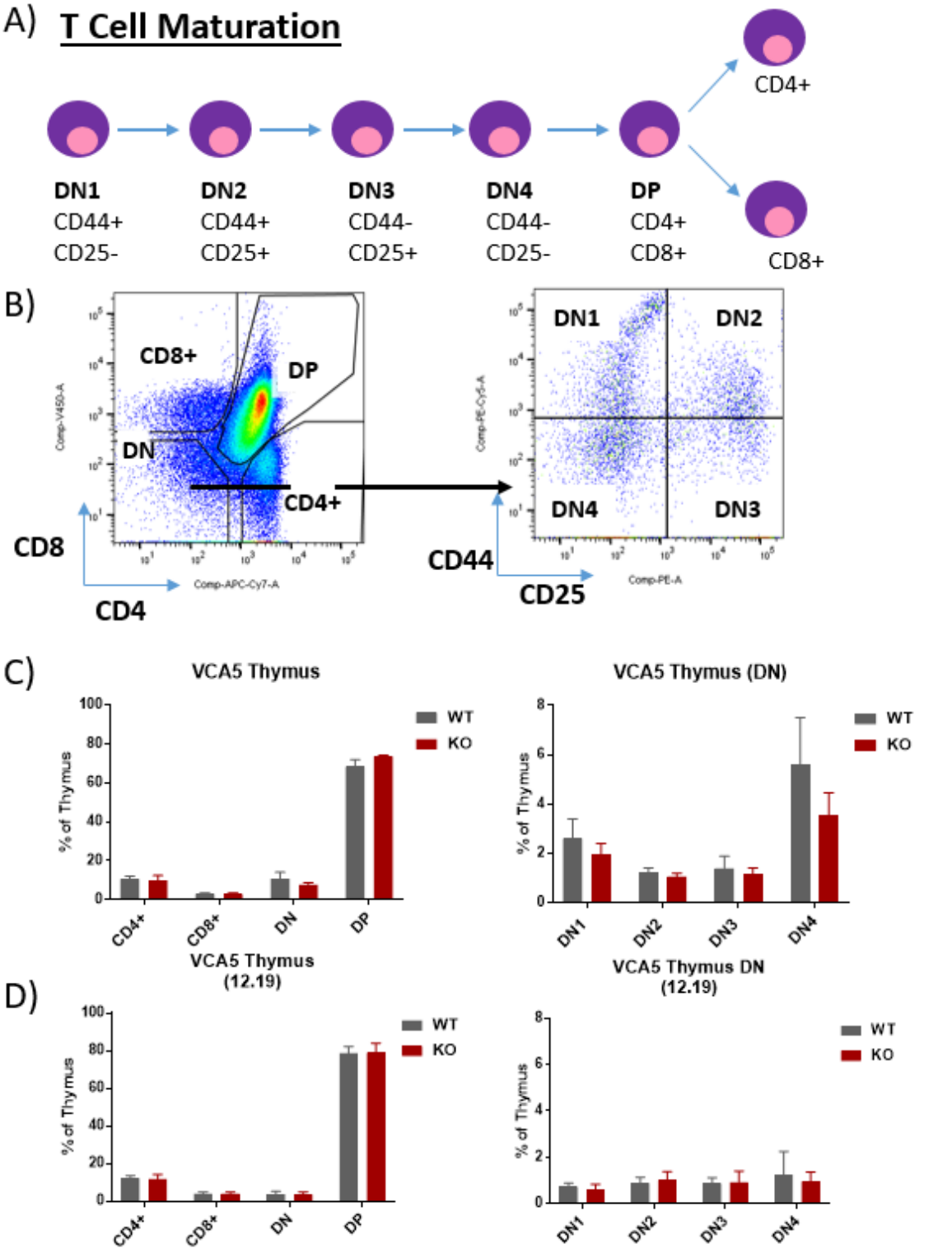

Figure 11: ***Characterization of T Cell development in VCA5 mice.*** A) Diagram illustrating T cell immunophenotype during maturation. DN: Double Negative; DP: Double Positive *Adapted from Fayard et al., 2010.* B) Gating schematic for identification of DP, CD8+, CD4+ and DN T Cells, as well as DN subsets. C) & D) Frequencies of T cell populations in 4-6 week old VCA5 mice. The two panels represent the results of two independent experiments (n=3 per group).

Next, we evaluated erythropoiesis using the same assessment of CD44 staining previously discussed. This revealed a trend towards decreased reticulocyte and mature RBC counts, but this was not statistically significant (Fig. 12). Moreover, complete blood counts performed on VCA5 KO mice did not exhibit anemia, and red blood cell indices did not differ significantly from WT (data not shown).

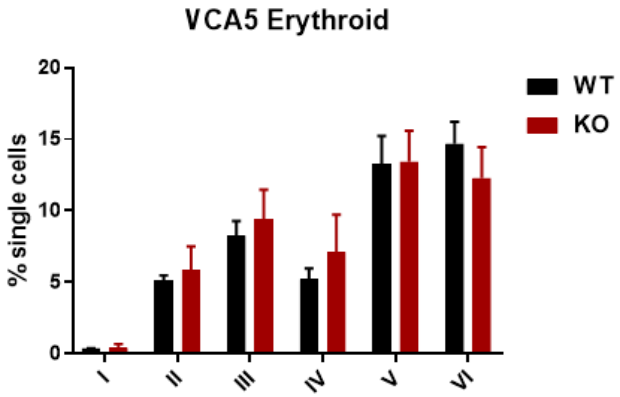

Figure 12: ***Erythropoiesis in 4-6 week old VCA5 mice.*** Erythroid development based on A) CD44 & Ter119 staining; B) Gating of erythrocyte precursors based on CD44 staining of Ter119+ erythrocytes, demonstrating Proerythroblasts (I), Basophilic Erythroblasts (II), Polychromatic Erythroblasts (III), Orthochromatic Erythroblasts (IV), Reticulocytes (V) and mature Red Blood Cells (VI) (n=3 per group).

Preserved Frequency and Colony-Forming Ability in VCA5 HSPCs

We next turned our attention to the HSPC compartment. Quantification of LSK cells in the bone marrow of 4-6 week old VCA5 mice in two independent experiments demonstrated no significant difference in LSK abundance between VCA5 WT & KO mice (Fig. 13A, B). To determine if VCA5 HSPCs maintained colony-forming ability in vitro, bone marrow cells harvested from individual VCA5 WT or KO mice were harvested and plated in triplicate for CFU assays. There was no difference in colony formation between VCA5 WT & KO cells (Figure 13 C, D).

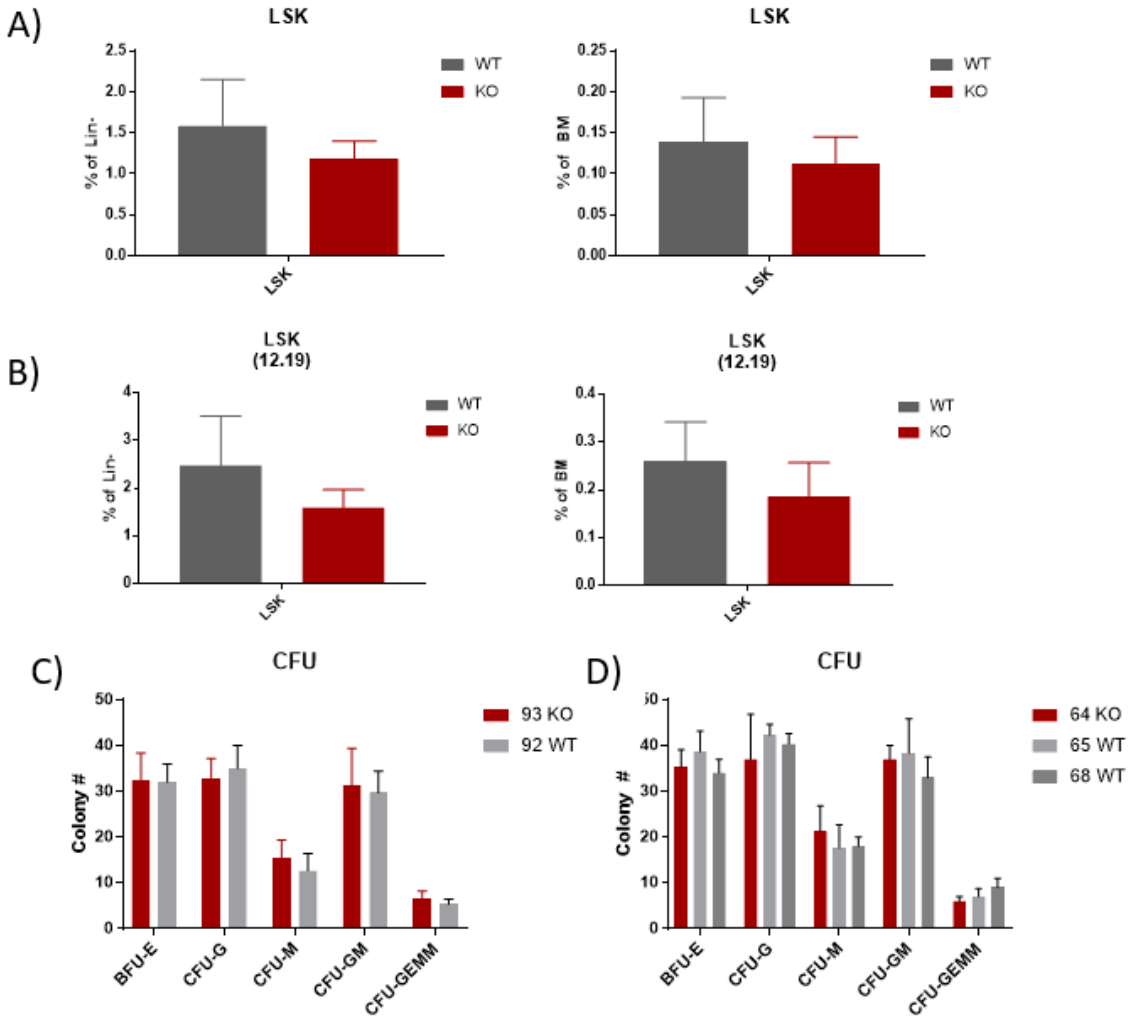

Figure 13: ***HSPC frequency & function in 4-6 week old VCA5 mice.***
A) & B) Bone marrow frequency of LSK as a percentage of Lin- bone marrow cells, and as a percentage of total bone marrow cellularity in VCA5 mice (n=3 per group). Results of two independent experiments.
C) & D) Colony forming unit (CFU) assays. Total bone marrow from littermate 4-6 week old VCA5 mice were plated in methylcellulose culture medium in triplicates, with colonies counted at day 14 (n=3 replicates per condition). Results of two independent experiments.

Diminished Chimerism of VCA5 KO Cells in Competitive Transplant

Given the apparently normal hematopoietic phenotype of VCA5 mice at steady state, we anticipated that VCA5 bone marrow would likely rescue hematopoiesis in lethally-irradiated recipients. We therefore elected to proceed with competitive transplantation to assess for subtler competitive advantages or disadvantages of VCA5 KO marrow compared to wildtype. We engrafted lethally-irradiated congenic CD45.1/2^{+} recipient mice with 0.5x10^{6} CD45.2^{+} VCM3 WT or KO fetal liver cells and an equal number of CD45.1^{+} competitor cells harvested from congenic Pep/3B mice, and then tracked engraftment of each donor population in the peripheral blood of recipient mice.

As expected, VCM3 WT marrow exhibited roughly 50% chimerism in the peripheral blood of recipient mice, reflecting the equal fitness of their HSPC compartment compared with that of competitor Pep/3B marrow. In contrast, peripheral blood chimerism of VCA5 KO donor marrow was drastically reduced, accounting for only ~20% of peripheral blood cells in the recipient mouse. These results were highly statistically significant, and were replicated in an independent experiment (Fig. 14A, 15A). To investigate the observed defects further, I assessed the relative frequencies myeloid and lymphoid cells within the CD45.2^{+} donor population. The relative frequencies of myeloid, B & T cells were similar in recipients receiving CD45.2^{+} VCA5 WT or KO marrow (Fig. 14B, C, D). While there were some small, statistically significant differences in lineage composition at individual time points in the first iteration of this experiment, they were not replicated in the second (Fig. 15B, C, D). Of note, these experiments are ongoing, with an intended 20-week total time-course.

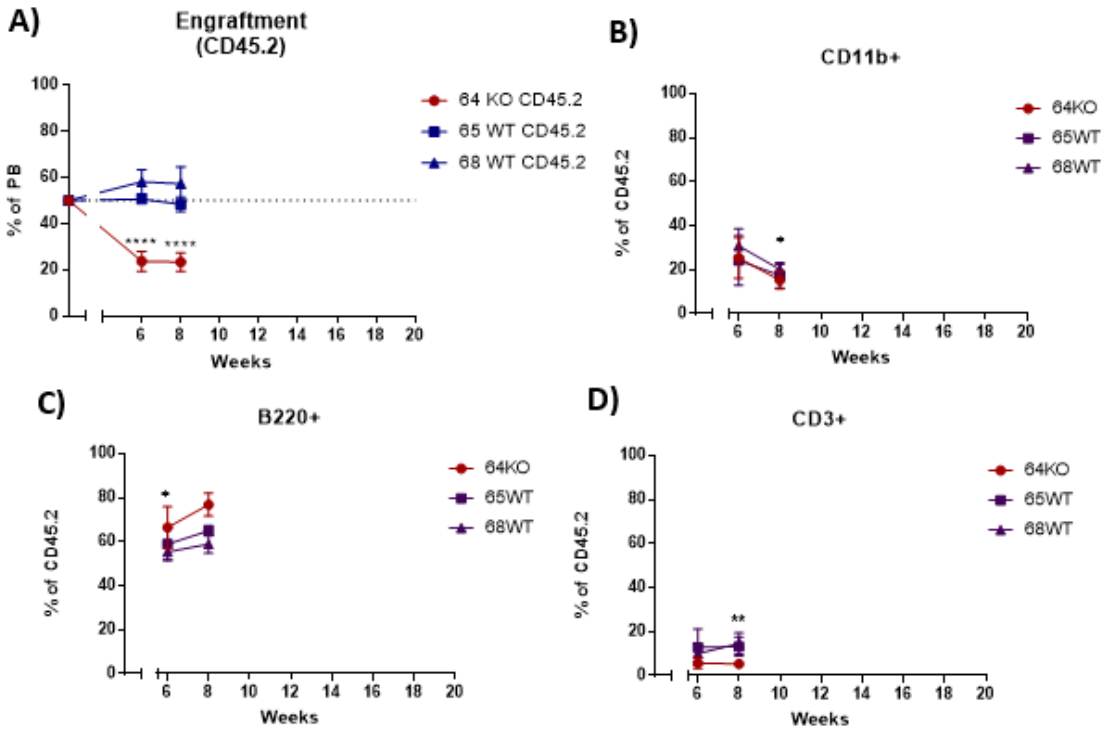

Figure 14: ***Competitive transplantation of VCA5 bone marrow.***
Recipient mice were lethally irradiated and received $5x10^5$ CD45.2 VCA5 KO (64 KO, n=6) or VCA5 WT(65WT, n=6; 68WT, n=5) bone marrow cells in competition with $5x10^5$ CD45.1 Pep3b bone marrow cells. A) Engraftment of CD45.2 cells in peripheral blood assessed by flow cytometry ($p<0.0001$). Dotted line indicates 50% engraftment.
Proportion of B) $CD11b^+$ myeloid cells ($p=0.0396$, 64KO vs 69WT) C) $B220^+$ B cells ($p=0.0363$; 64KO vs 68WT) and D) CD3+ T Cells ($p=0.0019$; 64KO vs 65WT) ($p=0.0017$; 64KO vs 68WT) within the donor $CD45.2^+$ population.

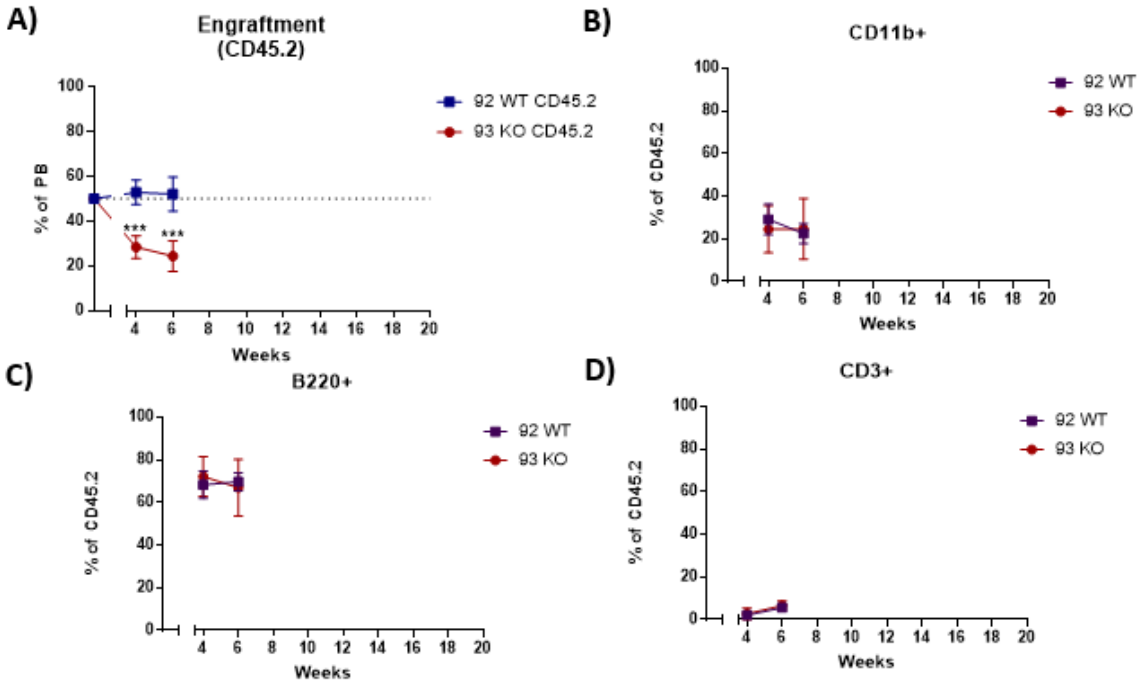

Figure 15*:* Results of repeat competitive transplantation assay. Recipient mice were lethally irradiated and received $5x10^5$ CD45.2 VCA5 KO (93 KO, n=5) or VCA5 WT (92 WT, n=4) bone marrow cells in competition with $5x10^5$ CD45.1 Pep3b bone marrow cells. A) Engraftment of CD45.2 cells in peripheral blood assessed by flow cytometry (p=0.0002 at week 4, p = 0.0007 at week 6). Dotted line indicates 50% engraftment.
Proportion of B) $CD11b^+$ myeloid cells (ns), C) $B220^+$ B cells (ns) and D) CD3+ T Cells (ns) within the donor $CD45.2^+$ population.

Overall, these findings imply that the HSPC compartment of VCA5 KO mice is impaired in its ability to reconstitute hematopoiesis in competition with wildtype donor marrow, but this difference is not attributable to specific defective contributions to mature myeloid or lymphoid lineages. Determining whether these findings correspond to homing defects, decreased engraftment of specific HSPC populations, or other deficiencies in self-renewal or differentiation will be the subject of future experiments.

Gene Expression Changes in VCM3 KO Mice

Having characterized prominent hematopoietic phenotypes in the VCM3 & VCA5 models, we proceeded to characterize gene expression changes in these mice by RNA-seq. We elected to focus our analysis on the HPSC compartment. To this end, we isolated LSK from VCM3 WT & VCM3 KO fetal liver by fluorescence activated cell sorting (FACS), from which we extracted total RNA, which was subsequently polyA-selected, and submitting for library preparation and sequencing. Sequencing of VCA5 LSK is pending.

RNA-sequencing revealed upregulated expression of 701 genes (KO_up), and downregulated expression of 1395 genes (KO_down) in VCM3 KO LSK cells (Fig. 16A, B).

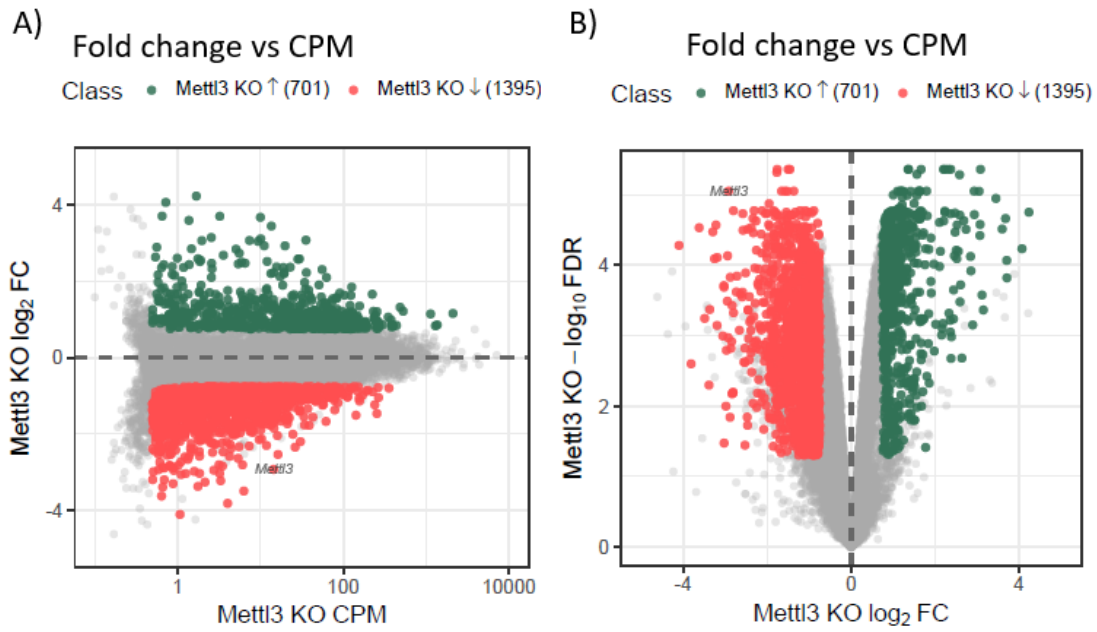

Figure 16*: **Expression changes in VCM3 KO Fetal Liver LSK by RNA-seq***. A) Transcript expression fold change (log_2 FC) in KO compared to WT, plotted against expression level (counts per million, CPM) in VCM3 KO. B) Significance of expression changes plotted as negative logarithm of false discovery rate (FDR) versus fold change (log_2 FC). METTL3 is highlighted in both plots. In both plots, genes that are significantly upregulated in VCM3 KO are green, and those that are downregulated are red.

METTL3 was >3-fold downregulated, confirming effective gene deletion. Interestingly, the methyltransferase components WTAP & RBM15 were upregulated, as was the m^{6}A reader YTHDF2.

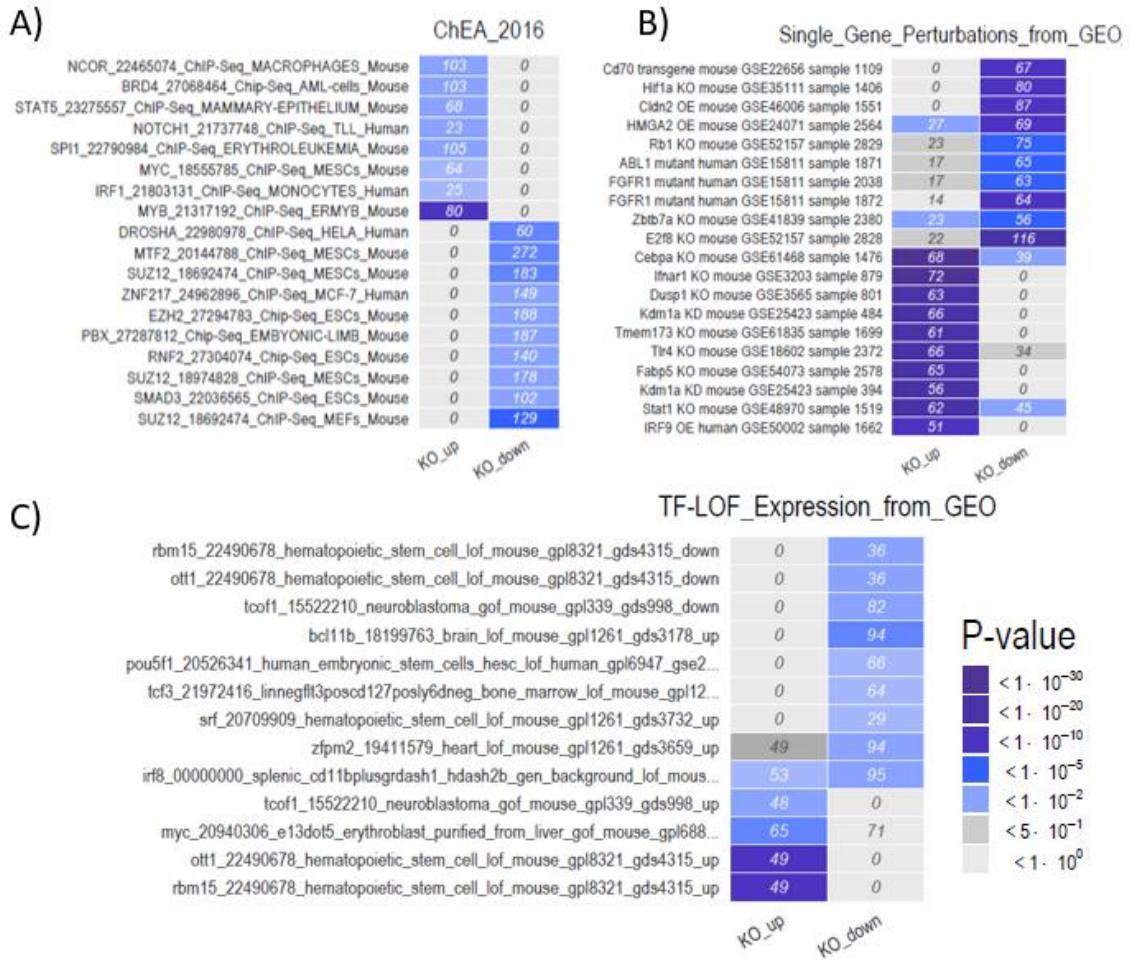

Figure 17*: Enrichment analyses of expression changes in VCM3 KO LSK.*
A) Enrichment of genes upregulated in VCM3 KO (KO_up) and genes downregulated in VCM3KO (KO_down) in chromatin immunoprecipitation (ChIP) data sets available in the ChEA enrichment analysis tool.
B) Enrichment of KO_up & KO_down genes amongst genes that are differentially downregulated in response to experimental manipulation of a single gene. OE indicates data sets in which the indicated genes were over-expressed, KO indicates knockout. Experimental data sets were drawn from the Gene Expression Omnibus (GEO) data sets.
C) Enrichment of KO_up & KO_down genes among genes that are differentially expressed in response to transcription factor loss of function. Experimental data sets were drawn from GEO.
Significance of enrichment is color-coded as described. Gene counts for non-significant findings were automatically set to zero.

Enrichment of Differentially Expressed Genes in ChIP Data Sets

To assess general pathways and processes that might be enriched within the differentially expressed genes observed in VCM3 KO LSK, we compared the list of differentially expressed genes to results from existing experimental data available from the Chromosome Enrichment Analysis (ChEA) tool, and the Gene Expression Omnibus (GEO) data sets.

We first searched for enrichment of our differentially regulated genes as targets of chromatin binding proteins based on available chromatin immunoprecipitation (ChIP) data (Fig. 17A). Consistent with previously published results, we found that upregulated genes in VCM3 KO (KO_up) were chromatin binding targets of STAT5[56], Notch1[72], SPI1[40], Myc[38,73] and Myb[40,73]. KO_up genes were also enriched for binding targets of the transcription factor NCOR, which functions upstream of Notch signaling in zebrafish to mediate HSC emergence in the AGM[90], and is mutated in MDS[91]. KO_up genes were also enriched for binding by BRD4, a chromatin reader protein that binds to acetyl-lysine and has been implicated as a therapeutic target in AML[92–94].

Genes that were downregulated in VCM3 KO (KO_down) were enriched for targets of DROSHA (Fig. 17A). This would be expected based on the interactions between METTL3 and the microprocessor machinery in miRNA biosynthesis[63,64], and could be consistent with the reported role of METTL3 in co-transcriptional gene silencing[48]. Interestingly, KO_down genes were enriched as targets of RNF2, MTF2, SUZ12, and EZH2. EZH2, SUZ12 and MTF are all of which are components of the Polycomb repressor complex 2 (PRC2). PRC2 mediates H3K27 trimethylation, which is a histone repressive mark important for gene silencing. RNF2 is an E3 ubiquitin ligase

and polycomb group protein that associates with PRC1 & PRC2[95]. Loss and gain of EZH2 occur in distinct hematopoietic malignancies[96,97], and it has been investigated as a therapeutic target in AML[98].

Genes that were differentially regulated by METTL3 and bound by EZH2, SUZ12 or RNF2 were frequently bound by multiple components of the polycomb machinery, increasing our confidence in their identity as potential PRC targets (Fig.18). Differentially regulated genes in VCM3 KO bound by two or more components of the polycomb machinery include CDKN2C, CDKN1C[99], Sox6, Pax5[100], Bach2[101], and Hoxa5, all of which have reported roles in hematopoiesis. This implies the possibility of METTL3-dependence of the PRC2 complex, which may correspond to hematopoietic phenotypes.

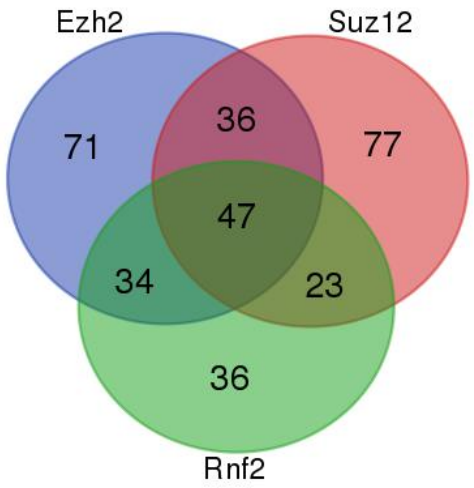

Figure 18*: **Mutual binding of differentially expressed genes in VCM3 KO LSK by Polycomb proteins.***
Venn diagram illustrating the number of differentially bound genes in VCM3 KO LSK as determined by RNA-seq that are bound by components of the Polycomb machinery.

Enrichment of Differentially Expressed Genes in Gene Perturbation Data Sets

We next examined RNA-seq data sets available from experiments in which the expression of single genes were perturbed by overexpression, mutation or knockout.

We first examined transcripts that were *downregulated* by experimental perturbation of individual genes in these data sets (Fig. 17B). We found that genes that were downregulated in response to Rb1 knockout, E2F8 knockout and ABL1 mutation were similarly downregulated by METTL3 deletion (KO_down). Genes that were downregulated in response to KDM1a knockdown were upregulated by METTL3 deletion (KO_up). Genes that were downregulated in response to CEBPα knockout or STAT1 knockout could be either KO_down or KO_up in VCM3 LSK (Fig. 17B).

We then examined RNA-seq data sets for transcripts that were *upregulated* in response to experimental gene perturbation. This showed that genes upregulated in response to Akt1 knockout, CEBPα knockout, or Myc knockout tend to be KO_down in VCM3 LSK, while genes upregulated in response to KDM1a also tend to be KO_up. (data not shown).

Akt, Myc and CEBPα have previously been implicated in METTL3 knockdown experiments in hematopoietic cells, while KDM1a represents a novel target. Rb1 and E2F8 interestingly synergize during terminal erythroid differentiation, and their absence results in anemia[87].

Enrichment of Differentially Expressed Genes in Transcription Factor LoF Data

Lastly we examined data sets in which transcription factor loss of function (LoF) experiments were performed for enrichment of VCM3 KO_up and KO_down genes.

Loss of RBM15 was synonymous with loss of METTL3 for a subset of targets, as genes which were upregulated in response to RBM15 LoF were exclusively upregulated in VCM3 KO, and those that were downregulated after RBM15 knockout were correspondingly downregulated in VCM3 KO (Fig. 17C). A small group of genes that were upregulated in response to SRF LoF were KO_down. Genes that were upregulated in response to Myc LoF could be either KO_up or KO_down.

The synonymous findings for RBM15 LoF and METTL3 KO are as expected, as RBM15 is a known methyltransferase component, which assists in the recruitment of METTL3 to specific targets. The perturbation of SRF targets in METTL3 KO is worth noting, as SRF1 is a transcription factor that is essential for megakaryopoiesis[102,103]. SRF is co-activated by MKL1/2 which, as mentioned previously, is one component of the RBM15-MKL fusion protein that occurs in acute megakaryoblastic leukemia[103,104].

Discussion

Here I have presented an initial phenotypic characterization of the VCM3 and VCA5 mice. In summary, VCM3 KO mice have a striking embryonic lethal phenotype, with an apparent increase in fetal liver LSK frequency, decreased myeloid progenitors with mildly increased mature myeloid cell production and defective erythropoiesis. Despite the increased LSK frequencies in VCM3 KO fetal liver, the HSPC compartment of these mice was defective in classic assays of self-renewal and differentiation. VCA5 mice appear to have no hematopoietic phenotype in steady-state, but are at a marked disadvantage in competitive transplant assays against wildtype bone marrow.

Apparent LSK Expansion in VCM3 KO Mice

From the current results, it is unclear whether transplanted VCM3 KO HSPCs persist in the recipient bone marrow and simply fail to proliferate and differentiate, or are eliminated over time. Unfortunately, we injected a small number of cells ($1x10^6$) during these transplant experiments, and did not analyze enough marrow cells to accurately assess the remaining number of donor HSCs post-transplant. We did confirm that there is no difference in HSPC engraftment between WT & KO cells at 16 hours following transplantation using fluorescent dyes. It would be of interest to perform similar fluorescent labeling and tracking experiments at later time points to assess the extent of wildtype compared to mutant proliferation. In future experiments we will have to assess entire marrow samples by flow cytometry to obtain a quantitative assessment of remaining cell numbers.

The expansion of the LSK compartment in VCM3 fetal livers coupled with their failure to rescue hematopoiesis in transplant experiments presents a compelling question.

It seems counterintuitive that a genetic alteration would simultaneously enforce HSC identity while preventing meaningful differentiation. Interesting analogies can be drawn to METTL3 deletion in other contexts. In the case of CD4+ T cells, METTL3 deletion leads to persistence in a naïve, undifferentiated state, with dramatically reduced proliferation following adoptive transfer. In this case, the phenotype is driven by a lack of responsiveness to cytokine signaling, as JAK/STAT signal transduction downstream of IL-7 is prevented by the persistence of SOCS gene expression in the absence of m^6A[56]. METTL3 deletion in murine embryonic stem cells results in a strikingly similar phenotype. These mESCs remained locked in a "ground" state, unable to resolve naïve pluripotency. As a consequence, knockout mESCs fail to contribute to meaningful chimera formation in embryo complementation assays and fail to form teratomas when injected into recipient mice. Weeks after injection into recipient mice for teratoma-forming assays, the mESCs can be retrieved and continue to propagate in culture, reflecting sustained self-renewal, and persistent pluripotency[51].

Our results examining VCM3 KO fetal liver HSPCs are reminiscent of the phenotypes of METTL3 knockout T cells and ESCs. Hematopoiesis ultimately fails, owing in part to defective differentiation, despite an increase in the immature LSK population. Pending analysis of larger amounts of bone marrow post-transplant may reveal persistence of transplanted, quiescent HSCs that tail to proliferate, similar to the persistently naïve METTL3 KO CD4+ T cells. Unfortunately there is no simple assay for HSC self-renewal. HSCs cannot be propagated in culture like ESCs, as they differentiate spontaneously within days. The theoretical gold standard assay for self-renewal is serial hematopoietic reconstitution in transplants, but this also depends on intact differentiation.

It is unclear which mechanisms may dictate this phenotype in HSCs – it is possible that, similar to T cells, m^6A-mediated responses to external cues such as cytokine signaling may be necessary for differentiation. In this case, the problem would be lack of response to an external pro-differentiation stimulus. Alternatively, VCM3 KO HSCs may rely on m^6A-mediated degradation of HSC-specific self-renewal transcripts for differentiation. In this case, the barrier to differentiation would be intrinsically enforced "stem-ness". RNA sequencing results from VCM3 WT & KO LSK cells are forthcoming, and may reveal whether one or both of these mechanisms is at play in HSPCs.

Decoupling HSC & Myeloid Phenotypes

In AML cell lines and human CD34+ cells, knockdown or knockout of METTL3 produces increased myeloid differentiation and abrogated leukemogenesis[38,73]. Loss of METTL14 similar results in myelopoiesis, and is negatively regulated by the core myeloid transcription factor PU.1[40]. How do we reconcile this apparently increased differentiation in cell lines with the increased fraction of immature LSK observed in our knockout mice? It is worth noting that in our VCM3 KO fetal liver, there is a small but statistically significant depletion of myeloid progenitors and increase in mature myeloid cells, which resembles the results of cell line experiments. Ultimately this apparent contradiction may depend on the extent to which human CD34+ cells and AML cell lines resemble immature HSCs as opposed to more committed progenitors. The cell of origin in AML, for instance, is thought to be a more committed myeloid progenitor which inappropriately gains the ability for self-renewal. AML cells are accordingly lineage restricted, and likely do not recapitulate a strong HSC identity. Similarly while CD34+

human samples are enriched for HSCs, they are highly heterogeneous. CD34 is expressed on all progenitor cells including CMP, GMP and MEP, and the bulk of patient samples are composed of these more frequent populations. As a result, the effects of METTL3 depletion on immature HSCs may be distinct from those seen in more committed myeloid progenitors. Loss of METTL3 may induce differentiation of myeloid progenitors, producing the observed increase in mature myeloid cells which we observe in VCM3 KO fetal liver, and which are seen in AML cells and CD34+ cells. However, it is also possible that more immature HSC-like cells are prevented from differentiating, as we see in the LSK compartment.

Of note, we have analyzed bone marrow from a small number of Mx1-Cre METTL3$^{f/f}$ (MCM3) mice following induction of Cre expression by pIpC injection. These mice exhibit a similar accumulation of immature LSK cells, and show prominent leukopenia and thrombocytopenia on complete blood count assays, rather than increased myeloid cell counts (data not shown). The MCM3 mice will provide a more robust model to assess the effect of METTL3 deletion on myelopoiesis over time, which is not possible in the fetal liver model. Furthermore, the adult marrow provides a more suitable system to assess the effect on myeloid differentiation, as myelopoiesis is a much more abundant process in the marrow than in the fetal liver.

Limitations to METTL3 as a Therapeutic Target

Given the overexpression of METTL3 in AML cell lines compared to normal hematopoietic tissue, there has been interest in targeting the methyltransferase therapeutically. METTL3 knockdown or knockout produce enhanced myeloid differentiation and abrogate leukemogenicity in mouse models. However, the prospects for METTL3 as a therapeutic target depend on the degree of AML cell dependence on m^6A, the level of toxicity caused by inhibition in normal tissues, and the ability to differentially target METTL3 in leukemic cells. Because METTL3 is a wildtype protein that is simply overexpressed, there is no basis for selectivity of drug effect towards METTL3 in leukemic cells as opposed to cells. It is therefore likely that any small molecule inhibitor of METTL3 would produce similar reductions in methyltransferase activity in diseased and normal cells, with a consequent likelihood of toxicity. It is theoretically possible that mild reductions in METTL3 activity could resolve differentiation blockade in leukemic cells, without inducing toxicity in normal tissues (i.e. a "therapeutic window"). However the experiments thus far have relied on high degrees of knockdown or complete knockout to achieve differentiation of AML cell lines. If complete loss of METTL3 is required for "therapeutic" effect, it is likely that toxicity would ensue from simultaneous inhibition of METTL3 in wildtype tissues. As the VCM3 mice demonstrate, METTL3 function is essential for normal hematopoiesis, and produces rapid embryonic lethality. Our early results from MCM3 mice suggest that they develop prominent cytopenias. It is therefore extremely likely that small molecule inhibitors of METTL3 would have a very narrow therapeutic window and small therapeutic index.

Attempts at developing therapeutics may be better targeted towards known upstream regulators of METTL3, or its downstream targets, which may produce more subtle effects. Upstream regulators include PU.1[40]. Downstream targets include Myc, Myb, SP1, and SP2[38,40,73]. Recently a novel therapeutic modality was developed for targeting Myb – this may be particularly effective in METTL3-overexpressing leukemia[105].

Stress Phenotype of VCA5 Mice

Disruption of the m^6A demethylase ALKBH5 in VCA5 mice produces a much more subtle phenotype than that seen in VCM3 fetal liver. This is in keeping with the established phenotype of constitutive knockout mice, which only exhibit deficiencies in spermatogenesis and fertility. As noted previously >90% of m^6A nucleotides are conserved between chromatin-associated and nucleoplasmic RNA, and >98% of m^6A sites are identical between nucleoplasmic and cytoplasmic RNA in HeLa cells at steady-state. These findings suggest m^6A demethylation may not play a meaningful physiologic role at steady state[45]. Nevertheless, marked remodeling of the epitranscriptome landscape is observed under stress conditions. A particularly well characterized example is during heat-shock, during which METTL3 re-localizes to specific targets, and YTHDF2 must be recruited to protect heat-shock transcripts from demethylation by FTO[48,49,60]. While the role of FTO as an m^6A demethylase remains the subject of debate, these findings potentially implicate the m^6A demethylases in adaptive cellular responses. Differentiation represents a cellular transition state mediated predominantly by epigenetic events. Cells in the hematopoietic hierarchy – with the special exception of B & T cells, which are subject to somatic recombination – share the same DNA content, but their identity is

dictated by distinctive patterns of gene expression, which are in turn controlled by DNA methylation, histone conformation, and distinct networks of transcription factor expression. Changes in RNA methylation may act as a necessary event during differentiation, as is the case during the resolution of naïve pluripotency in embryonic stem cells[51]. While absence of ALKBH5 is clearly not a barrier to establishing an intact hematopoietic system, the deficiencies of VCA5 KO mice compared to wildtype in competitive transplant assays may be an indication of developmental rigidity and delay in dynamic responses to hematopoietic stress. We intend to explore this possibility further by subjecting VCA5 mice to stressors such as chemotherapy treatment with 5-fluorouracil or phlebotomy. The relatively mild phenotype of the VCA5 mice may also be due to compensation of demethylase activity by FTO or other potentially unknown m^6A demethylases. In this regard, examination of ALKBH5 & FTO double-knockouts may be of interest. It will be important to exclude homing defects as an underlying cause for the in competitive transplant phenotype, as we did in the case of VCM3 transplants. It is worth noting that spermatogenesis, the sole area in which VCA5 mice appear deficient, represents a similar epigenetic transition as the germline must be wiped clean of key epigenetic marks in anticipation of an eventual fertilization event.

Possible Mechanisms of METTL3 Function in Hematopoiesis

Our RNA sequencing data provide a glimpse at potential mechanisms that may underlie the hematopoietic phenotypes observed in VCM3 KO fetal liver. Importantly, differential expression at the transcript level does not always correlate to protein level alterations, and we will need to perform ribosomal profiling to determine the translational efficiency of target transcripts. We will similarly need to perform miCLIP to determine which changes in transcript-level expression are accounted for by m^6A methylation, and which are a result of secondary effects. Nevertheless, these preliminary data merit discussion.

As outlined briefly in the results, differentially expressed genes identified in RNA-sequencing of VCM3 KO fetal liver LSK were enriched as targets of chromatin-binding proteins with known roles in hematopoiesis. Several differentially expressed genes in VCM3 KO were mutually regulated by important hematopoietic transcription factors, signaling proteins and epigenetic modifiers.

Differentially regulated VCM3 KO transcripts were enriched for targets of the chromatin reading enzyme BRD4, as identified by ChIP. BRD4 is a bromodomain protein that mediates assembly of transcription factors near acetylate histones with a tendency towards enhancement of transcription[92]. Small molecule inhibitors of BRD4 have been applied to the treatment of various subtypes of AML, including in those with MLL rearrangements[94]. Leukemia with IDH2 mutations also appear susceptible to BRD4 inhibition[93]. If the pro-differentiation effects of METTL3 depletion observed in AML cell lines are in part mediated by inhibition of BRD4, then METTL3 overexpression could be used as a biomarker for sensitivity to BRD4 inhibitors. BRD4 target transcripts are

upregulated in VCM3 KO, which suggests that METTL3 deletion does not pheno-copy BRD4 inhibition, as we might expect transcriptional repression of BRD4 targets. However, it is important to note that inhibition of BRD4 does not necessarily have straightforward inhibitory effects on transcription. As a result, a role for BRD4 in METTL3 overexpressing AML is still a possibility worth considering.

Genes that were downregulated in VCM3 KO LSK (KO_down) were interestingly enriched for targets of EZH2, SUZ12 RNF2, and MTF2 in ChIP Data. EZH2 & SUZ12 are two of the core components of the Polycomb Repressor Complex 2 (PRC2). As discussed previously, PRC2 deposits the H3K27me3 repressive histone modification, which is responsible for durable silencing of gene expression. MTF2 is a non-constitutive element of PRC2[106], and RNF2 is also a polycomb protein. PRC2 is known to be necessary for ESC differentiation[107,108], and is implicated in hematopoiesis and myeloid malignancies[96,98]. The fact that PRC2 targets were uniformly downregulated in VCM3 KO LSK suggests that METTL3 may normally function to prevent silencing of gene expression by PRC2. Two possible mechanisms for this function are conceivable. First, given that METTL3 is known to interact directly with chromatin[38,48], it could either directly antagonize PRC2 binding or mediate local effects at target DNA sequences to maintain an open chromatin conformation and prevent PRC2 binding (Fig. 19A). Alternatively, METTL3 inhibition of PRC2 could be dependent on m^6A RNA. Recent evidence shows that the recruitment of PRC2 to target DNA can be directly inhibited by RNA[109]. In this case, RNA acts as a competitive decoy, as PRC2 binding to RNA or DNA is mutually exclusive. It is conceivable that RNA binding to PRC2 is dependent on

m^6A methylation of the target RNA substrate (Fig. 19B). This would provide a fascinating link between the epitranscriptome and epigenome.

To examine this possibility further, we will assess distribution of H3K27me3 and PRC2 in VCM3 fetal liver by immunofluorescence and ChIP. We can further assess whether METTL3 binds directly to potential PRC2 targets by examining existing METTL3 ChIP data. If this effect does not appear to be mediated by chromatin-binding of METTL3, then the RNA-mediated mechanism could be investigated by biochemical assays.

A final possible molecular mechanism that may explain part of the VCM3 fetal liver phenotype based on our preliminary RNA-seq data involves Rb & E2F8. Rb is a well-known tumor suppressor, and both Rb & E2F8 are involved in cell cycle regulation. Knockdown of either Rb or E2F8 results in downregulation of a set of transcripts that are also downregulated in VCM3 KO LSK, as discussed in the results. Compellingly, Rb and E2F8 normally function synergistically to promote terminal erythroid differentiation, and loss of either protein results in aberrant erythropoiesis and anemia[87], similar to what we have observed in VCM3 fetal liver and in preliminary analyses of MCM3 adult marrow. It is possible that METTL3 is necessary for appropriate function of Rb & E2F8. This developmental axis may therefore account for the erythropoietic phenotype observed in VCM3 fetal liver, and would merit further investigation if it is supported by forthcoming miCLIP and ribosomal sequencing data.

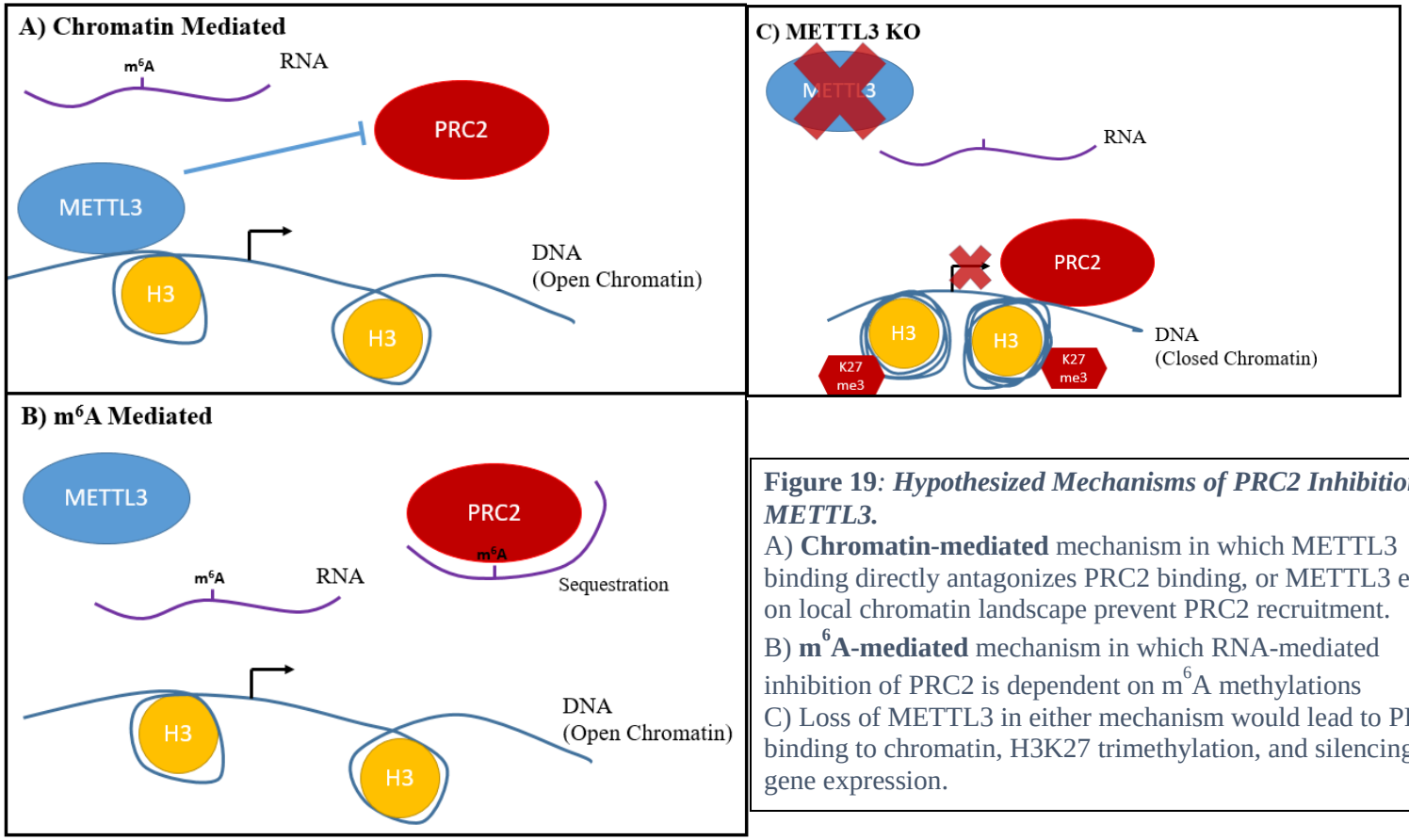

Figure 19: ***Hypothesized Mechanisms of PRC2 Inhibition by METTL3.***
A) **Chromatin-mediated** mechanism in which METTL3 binding directly antagonizes PRC2 binding, or METTL3 effects on local chromatin landscape prevent PRC2 recruitment.
B) **m^{6}A-mediated** mechanism in which RNA-mediated inhibition of PRC2 is dependent on m^{6}A methylations
C) Loss of METTL3 in either mechanism would lead to PRC2 binding to chromatin, H3K27 trimethylation, and silencing of gene expression.

Limitations of the Present Findings, and Future Experiments

It is important to acknowledge that the present findings are limited in scope, and represent only a preliminary characterization of VCM3 and VCA5 mice, with mechanistic studies forthcoming.

First and foremost, many of the findings are limited by the small sample number. This is admittedly due to the difficult nature of fetal liver characterization. This process relies on time mating and analysis two weeks later. We are therefore dependent on the yield of desirable genotypes within any given litter, and with a probability of only 12.5% in our crossings, knockout mice are infrequent. Many of the observed trends in our phenotypic data will likely attain significance with increased numbers.

Mechanistically, it will be important to quantify the m^6A content of these knockout mice by liquid-chromatography/mass-spectrometry to verify that altered m^6A levels are caused by deletion of these genes. In the case of the VCM3 mice, several studies have demonstrated that knockdown or knockout of METTL3 induces dramtic reductions in m^6A. The floxed METTL3 construct in these mice is the same that was used in the previously published characterization of CD4 T cells, and Vav is a well-characterized promoter that mediates efficient Cre expression in hematopoietic tissues. We therefore expect efficient deletion and altered m^6A levels. In ALKBH5 knockout mice, there is only a mild increase in total m^6A content. Furthermore, alterations in m^6A levels in VCA5 may be transient or context-dependent, and may be more difficult to detect. We will also demonstrate that the observed phenotypes can be reversed by rescue of METTL3 and ALKBH5 expression. We will also have to demonstrate that rescue by

METTL3 and ALKBH5 is dependent on their m^6A-specific function by performing rescue with catalytically inactive mutants.

Beyond these core experiments, we will also have to explore the causal alterations in the epitranscriptome, and translational efficiency that are mediated by METTL3 and ALKBH5 knockout, as outlined in the aims of this project. As discussed at length previously, large cell numbers will be required for miCLIP and ribosomal profiling. To this end we will consider performing these studies on whole fetal liver, or on the Lin^- $cKit^+$ fractions.

Lastly, as evidence continues to emerge regarding the role of METTL3 in hematopoiesis, it will be important to demonstrate novel mechanisms and identify novel targets in our current model.

References

1. Cazzola, M., Della Porta, M. G. & Malcovati, L. The genetic basis of myelodysplasia and its clinical relevance. *Blood* **122,** 4021–34 (2013).
2. Tefferi, A. & Vardiman, J. W. Myelodysplastic syndromes. *N. Engl. J. Med.* **361,** 1872–85 (2009).
3. Sperling, A. S., Gibson, C. J. & Ebert, B. L. The genetics of myelodysplastic syndrome: from clonal haematopoiesis to secondary leukaemia. *Nat. Rev. Cancer* **advance on,** 5–19 (2016).
4. Arber, D. A. *et al.* The 2016 revision to the World Health Organization classi fi cation of myeloid neoplasms and acute leukemia. *Blood* **127,** 2391–2406 (2016).
5. Bejar, R. & Steensma, D. P. Recent developments in myelodysplastic syndromes. **124,** 2793–2804 (2014).
6. Fenaux, P. & Ad, L. How I Treat How we treat lower-risk myelodysplastic syndromes. **121,** 4280–4287 (2018).
7. Krönke, J. *et al.* Lenalidomide induces ubiquitination and degradation of CK1α in del(5q) MDS. *Nature* **523,** 183–188 (2015).
8. Fenaux, P. *et al.* Efficacy of azacitidine compared with that of conventional care regimens in the treatment of higher-risk myelodysplastic syndromes: a randomised, open-label, phase III study. *Lancet Oncol.* **10,** 223–232 (2009).
9. Silverman, L. R. *et al.* Randomized controlled trial of azacitidine in patients with the myelodysplastic syndrome: A study of the cancer and leukemia group B. *J. Clin. Oncol.* **20,** 2429–2440 (2002).
10. Lübbert, M. *et al.* Low-Dose Decitabine Versus Best Supportive Care in Elderly Patients With Intermediate-or High-Risk Myelodysplastic Syndrome (MDS) Ineligible for Intensive Chemotherapy: Final Results of the Randomized Phase III Study of the European Organisation for Research and Treatment of Cancer Leukemia Group and the German MDS Study Group. *J Clin Oncol* **29,** 1987–1996
11. Kröger, N. Allogeneic stem cell transplantation for elderly patients with myelodysplastic syndrome. *Blood* **119,** 5632–5639 (2012).
12. Lindsley, R. C. *et al.* Acute myeloid leukemia ontogeny is de fi ned by distinct somatic mutations. **125,** 1367–1377 (2015).
13. Steensma, D. P. *et al.* Clonal hematopoiesis of indeterminate potential and its distinction from myelodysplastic syndromes. *Blood* **126,** 9–16 (2015).
14. Jaiswal, S. *et al.* Age-Related Clonal Hematopoiesis Associated with Adverse Outcomes. *N. Engl. J. Med.* **371,** 2488–2498 (2014).
15. Jaiswal, S. *et al.* Clonal Hematopoiesis and Risk of Atherosclerotic Cardiovascular Disease. *N. Engl. J. Med.* **377,** 111–121 (2017).
16. Yoshida, K. *et al.* Frequent pathway mutations of splicing machinery in myelodysplasia. *Nature* **478,** 64–9 (2011).
17. Haferlach, T. *et al.* Landscape of genetic lesions in 944 patients with myelodysplastic syndromes. *Leukemia* **28,** 241–7 (2014).
18. Mardis, E. R. *et al.* Recurring mutations found by sequencing an acute myeloid leukemia genome. *N. Engl. J. Med.* **361,** 1058–66 (2009).
19. Marcucci, G. *et al.* IDH1 and IDH2 gene mutations identify novel molecular subsets within de novo cytogenetically normal acute myeloid leukemia: A cancer

and leukemia group B study. *J. Clin. Oncol.* **28,** 2348–2355 (2010).
20. Figueroa, M. E. *et al.* Leukemic IDH1 and IDH2 Mutations Result in a Hypermethylation Phenotype, Disrupt TET2 Function, and Impair Hematopoietic Differentiation. *Cancer Cell* **18,** 553–567 (2010).
21. Parsons, D. W. *et al.* An Integrated Genomic Analysis of. *Science (80-.).* **1807,** 1807–1813 (2010).
22. Dang, L. *et al.* Cancer-associated IDH1 mutations produce 2-hydroxyglutarate. *Nature* **462,** 739–44 (2009).
23. Ward, P. S. *et al.* The Common Feature of Leukemia-Associated IDH1 and IDH2 Mutations Is a Neomorphic Enzyme Activity Converting ??-Ketoglutarate to 2-Hydroxyglutarate. *Cancer Cell* **17,** 225–234 (2010).
24. Lu, C., Ward, P., Kapoor, G. & Rohle, D. IDH mutation impairs histone demethylation and results in a block to cell differentiation. *Nature* **483,** 474–478 (2012).
25. Wang, P. *et al.* Oncometabolite D-2-Hydroxyglutarate Inhibits ALKBH DNA Repair Enzymes and Sensitizes IDH Mutant Cells to Alkylating Agents. *Cell Rep.* **13,** 2353–2361 (2015).
26. Desrosiers, R., Friderici, K. & Rottman, F. Identification of methylated nucleosides in messenger RNA from Novikoff hepatoma cells. *Proc. Natl. Acad. Sci. U. S. A.* **71,** 3971–5 (1974).
27. Jia, G. *et al.* N6-methyladenosine in nuclear RNA is a major substrate of the obesity-associated FTO. *Nat. Chem. Biol.* **7,** 885–7 (2011).
28. Zheng, G. *et al.* ALKBH5 Is a Mammalian RNA Demethylase that Impacts RNA Metabolism and Mouse Fertility. *Mol. Cell* **49,** 18–29 (2013).
29. Meyer, K. D. *et al.* Comprehensive analysis of mRNA methylation reveals enrichment in 3′ UTRs and near stop codons. *Cell* **149,** 1635–1646 (2012).
30. Dominissini, D. *et al.* Topology of the human and mouse m6A RNA methylomes revealed by m6A-seq. *Nature* **485,** 201–206 (2012).
31. Dominissini, D., Moshitch-Moshkovitz, S., Salmon-Divon, M., Amariglio, N. & Rechavi, G. Transcriptome-wide mapping of N(6)-methyladenosine by m(6)A-seq based on immunocapturing and massively parallel sequencing. *Nat. Protoc.* **8,** 176–89 (2013).
32. Schwartz, S. *et al.* Perturbation of m6A writers reveals two distinct classes of mRNA methylation at internal and 5' sites. *Cell Rep.* **8,** 284–296 (2014).
33. Linder, B. *et al.* Single-nucleotide-resolution mapping of m6A and m6Am throughout the transcriptome. *Nat Methods* **12,** 767–772 (2015).
34. Mauer, J. *et al.* Reversible methylation of m6Am in the 5′ cap controls mRNA stability. *Nature* **541,** 371–375 (2016).
35. Elkashef, S. M. *et al.* IDH Mutation, Competitive Inhibition of FTO, and RNA Methylation. *Cancer Cell* **31,** 619–620 (2017).
36. Li, Z. *et al.* FTO Plays an Oncogenic Role in Acute Myeloid Leukemia as a N6-Methyladenosine RNA Demethylase. *Cancer Cell* **31,** 127–141 (2016).
37. Xu, W. *et al.* Oncometabolite 2-hydroxyglutarate is a competitive inhibitor of ??-ketoglutarate-dependent dioxygenases. *Cancer Cell* **19,** 17–30 (2011).
38. Barbieri, I. *et al.* Promoter-bound METTL3 maintains myeloid leukaemia by m6A-dependent translation control. *Nature* (2017). doi:10.1038/nature24678

39. Vu, L. P. *et al.* The N6-methyladenosine (m6A)-forming enzyme METTL3 controls myeloid differentiation of normal hematopoietic and leukemia cells. *Nat. Med.* (2017). doi:10.1038/nm.4416
40. Weng, H. *et al.* METTL14 Inhibits Hematopoietic Stem/Progenitor Differentiation and Promotes Leukemogenesis via mRNA m 6 A Modification. *Cell Stem Cell* 1–15 (2017). doi:10.1016/j.stem.2017.11.016
41. Patil, D. P. *et al.* m6A RNA methylation promotes XIST-mediated transcriptional repression. *Nature* **537,** 1–25 (2016).
42. Ayllón, V. *et al.* New hPSC-based human models to study pediatric Acute Megakaryoblastic Leukemia harboring the fusion oncogene RBM15-MKL1. *Stem Cell Res.* **19,** 1–5 (2017).
43. Licatalosi, D. D. *et al.* HITS-CLIP yields genome-wide insights into brain alternative RNA processing. *Nature* **456,** 464–469 (2008).
44. König, J. *et al.* ICLIP reveals the function of hnRNP particles in splicing at individual nucleotide resolution. *Nat. Struct. Mol. Biol.* **17,** 909–915 (2010).
45. Ke, S. *et al.* A majority of m ^{6} A residues are in the last exons, allowing the potential for 3′ UTR regulation. *Genes Dev.* **29,** 2037–2053 (2015).
46. Ke, S. *et al.* m6A mRNA modifications are deposited in nascent pre-mRNA and are not required for splicing but do specify cytoplasmic turnover. *Genes Dev.* **31,** 990–1006 (2017).
47. Rosa-Mercado, N. A., Withers, J. B. & Steitz, J. A. Settling the m6A debate: Methylation of mature mRNA is not dynamic but accelerates turnover. *Genes Dev.* **31,** 957–958 (2017).
48. Knuckles, P. *et al.* RNA fate determination through cotranscriptional adenosine methylation and microprocessor binding. *Nat. Publ. Gr.* (2017). doi:10.1038/nsmb.3419
49. Zhou, J. *et al.* Dynamic m(6)A mRNA methylation directs translational control of heat shock response. *Nature* **526,** 591–594 (2015).
50. Baudin-Baillieu, A., Hatin, I., Legendre, R. & Namy, O. in *Methods in Molecular Biology* **1361,** 105–124 (2016).
51. Geula, S. *et al.* m6A mRNA methylation facilitates resolution of naive pluripotency toward differentiation. *Science (80-.).* **347,** 1002–1006 (2015).
52. Wang, X. *et al.* N6-methyladenosine-dependent regulation of messenger RNA stability. *Nature* **505,** 117–20 (2014).
53. Wang, Y. *et al.* N6-methyladenosine modification destabilizes developmental regulators in embryonic stem cells. *Nat. Cell Biol.* **16,** 191–8 (2014).
54. Chen, T. *et al.* M6A RNA methylation is regulated by microRNAs and promotes reprogramming to pluripotency. *Cell Stem Cell* **16,** 289–301 (2015).
55. Batista, P. J. *et al.* M^{6}A RNA modification controls cell fate transition in mammalian embryonic stem cells. *Cell Stem Cell* **15,** 707–719 (2014).
56. Li, H.-B. *et al.* m6A mRNA methylation controls T cell homeostasis by targeting the IL-7/STAT5/SOCS pathways. *Nature* **548,** 338–342 (2017).
57. Yoon, K. J. *et al.* Temporal Control of Mammalian Cortical Neurogenesis by m6A Methylation. *Cell* 1–13 (2017). doi:10.1016/j.cell.2017.09.003
58. Adhikari, S., Xiao, W., Zhao, Y.-L. & Yang, Y.-G. m(6)A: Signaling for mRNA splicing. *RNA Biol.* **6286,** 1–4 (2016).

59. Wang, X. *et al.* N^6-methyladenosine modulates messenger RNA translation efficiency. *Cell* **161,** 1388–1399 (2015).
60. Meyer, K. D. *et al.* 5??? UTR m6A Promotes Cap-Independent Translation. *Cell* **163,** 999–1010 (2015).
61. Mauer, J. *et al.* Reversible methylation of m6Amin the 5′ cap controls mRNA stability. *Nature* **541,** 371–375 (2017).
62. Winter, J., Jung, S., Keller, S., Gregory, R. I. & Diederichs, S. Many roads to maturity: MicroRNA biogenesis pathways and their regulation. *Nature Cell Biology* **11,** 228–234 (2009).
63. Alarcón, C. R., Lee, H., Goodarzi, H., Halberg, N. & Tavazoie, S. F. N6-methyladenosine marks primary microRNAs for processing. *Nature* **519,** 482–5 (2015).
64. Alarcón, C. R. *et al.* HNRNPA2B1 Is a Mediator of m6A-Dependent Nuclear RNA Processing Events. *Cell* 1299–1308 (2015). doi:10.1016/j.cell.2015.08.011
65. Meyer, K. D. & Jaffrey, S. R. Rethinking m ^{6} A Readers, Writers, and Erasers. *Annu. Rev. Cell Dev. Biol.* **33,** 319–342 (2017).
66. Martinez, F. J. *et al.* Protein-RNA Networks Regulated by Normal and ALS-Associated Mutant HNRNPA2B1 in the Nervous System. *Neuron* **92,** 780–795 (2016).
67. Zhao, X. *et al.* FTO-dependent demethylation of N6-methyladenosine regulates mRNA splicing and is required for adipogenesis. *Cell Res.* **24,** 1403–19 (2014).
68. Xiao, W. *et al.* Nuclear m6A Reader YTHDC1 Regulates mRNA Splicing. *Mol. Cell* **61,** 507–519 (2016).
69. Teofili, L. *et al.* Epigenetic alteration of SOCS family members is a possible pathogenetic mechanism in JAK2 wild type myeloproliferative diseases. *Int. J. Cancer* **123,** 1586–1592 (2008).
70. Usenko, T. *et al.* Overexpression of SOCS-2 and SOCS-3 genes reverses erythroid overgrowth and IGF-I hypersensitivity of primary polycythemia vera (PV) cells. *Leuk. Lymphoma* **48,** 134–146 (2007).
71. Sasaki, A. *et al.* CIS3/SOCS-3 suppresses erythropoietin (EPO) signaling by binding the EPO receptor and JAK2. *J. Biol. Chem.* **275,** 29338–29347 (2000).
72. Zhang, C. *et al.* m6A modulates haematopoietic stem and progenitor cell specification. *Nature* **549,** 273–276 (2017).
73. Vu, L. P. *et al.* The N 6 -methyladenosine (m 6 A)-forming enzyme METTL3 controls myeloid differentiation of normal hematopoietic and leukemia cells. *Nat. Med.* **23,** 1369–1376 (2017).
74. Li, Z. *et al.* FTO Plays an Oncogenic Role in Acute Myeloid Leukemia as a N6-Methyladenosine RNA Demethylase. *Cancer Cell* **31,** 127–141 (2017).
75. Su, R. *et al.* R-2HG Exhibits Anti-tumor Activity by Targeting FTO/m6A/MYC/CEBPA Signaling. *Cell* 1–16 (2017). doi:10.1016/j.cell.2017.11.031
76. Sulkowski, P. L. *et al.* 2-Hydroxyglutarate produced by neomorphic IDH mutations suppresses homologous recombination and induces PARP inhibitor sensitivity. **2463,** (2017).
77. Inoue, S. *et al.* Mutant IDH1 Downregulates ATM and Alters DNA Repair and Sensitivity to DNA Damage Independent of TET2. *Cancer Cell* **30,** 337–348

(2016).
78. Amatangelo, M. D. *et al.* Enasidenib induces acute myeloid leukemia cell differentiation to promote clinical response. *Blood* **130,** 732–741 (2017).
79. Stein, E. M. *et al.* Enasidenib in mutant *IDH2* relapsed or refractory acute myeloid leukemia. *Blood* **130,** 722–731 (2017).
80. Speck, N. A. & Iruela-Arispe, M. L. Conditional Cre/LoxP strategies for the study of hematopoietic stem cell formation. *Blood Cells, Mol. Dis.* **43,** 6–11 (2009).
81. Joseph, C. *et al.* Deciphering Hematopoietic Stem Cells in Their Niches: A Critical Appraisal of Genetic Models, Lineage Tracing, and Imaging Strategies. *Cell Stem Cell* **13,** 520–533 (2013).
82. Oguro, H., Ding, L. & Morrison, S. J. SLAM family markers resolve functionally distinct subpopulations of hematopoietic stem cells and multipotent progenitors. *Cell Stem Cell* **13,** 102–116 (2013).
83. Wang, G. G. *et al.* Quantitative production of macrophages or neutrophils ex vivo using conditional Hoxb8. *Nat. Methods* **3,** 287–293 (2006).
84. Sykes, D. B. *et al.* Inhibition of Dihydroorotate Dehydrogenase Overcomes Differentiation Blockade in Acute Myeloid Leukemia. *Cell* **167,** 171–186.e15 (2016).
85. Laurenti, E. & Göttgens, B. Review From haematopoietic stem cells to complex differentiation landscapes. *Nat. Publ. Gr.* **553,** 418–426 (2018).
86. Welch, J. S. *et al.* The origin and evolution of mutations in acute myeloid leukemia. *Cell* **150,** 264–78 (2012).
87. Liu, J. *et al.* Quantitative analysis of murine terminal erythroid differentiation in vivo: novel method to study normal and disordered erythropoiesis. doi:10.1182/blood-2012
88. Fayard, E., Moncayo, G., Hemmings, B. A. & Holländer, G. A. Phosphatidylinositol 3-kinase signaling in thymocytes: The need for stringent control. *Sci. Signal.* **3,** 1–13 (2010).
89. Saba, I., Kosan, C., Vassen, L. & Mo, T. IL-7R – dependent survival and differentiation of early T-lineage progenitors is regulated by the BTB / POZ domain transcription factor Miz-1. **117,** 3370–3381 (2011).
90. Wei, Y. *et al.* Ncor2 is required for hematopoietic stem cell emergence by inhibiting Fos signaling in zebrafish. *Blood* **124,** 1578–1585 (2014).
91. Gill, H., Leung, A. & Kwong, Y.-L. Molecular and Cellular Mechanisms of Myelodysplastic Syndrome: Implications on Targeted Therapy. *Int. J. Mol. Sci.* **17,** 440 (2016).
92. Roe, J.-S. & Vakoc, C. R. The Essential Transcriptional Function of BRD4 in Acute Myeloid Leukemia. *Cold Spring Harb. Symp. Quant. Biol.* **LXXXI,** 31039 (2017).
93. Chen, C. *et al.* Cancer-associated IDH2 mutants drive an acute myeloid leukemia that is susceptible to Brd4 inhibition. *Genes Dev.* **27,** 1974–1985 (2013).
94. Gilan, O. *et al.* Functional interdependence of BRD4 and DOT1L in MLL leukemia. *Nat. Struct. Mol. Biol.* **23,** (2016).
95. Wang, Z. *et al.* A Non-canonical BCOR-PRC1.1 Complex Represses Differentiation Programs in Human ESCs. *Cell Stem Cell* **22,** 235–251.e9 (2018).
96. Khan, S. N. *et al.* Multiple mechanisms deregulate EZH2 and histone H3 lysine 27

epigenetic changes in myeloid malignancies. *Leukemia* **27,** 1301–9 (2013).
97. Thol, F. *et al.* Acute myeloid leukemia derived from lympho-myeloid clonal hematopoiesis. *Leukemia* **31,** 1286–1295 (2017).
98. Fujita, S. *et al.* Dual inhibition of EZH1/2 breaks the quiescence of leukemia stem cells in acute myeloid leukemia. *Nat. Publ. Gr.* (2017). doi:10.1038/leu.2017.300
99. Zhang, Y. *et al.* PR-domain - containing Mds1-Evi1 is critical for long-term hematopoietic stem cell function. *Blood* **118,** 3853–3861 (2011).
100. Somasundaram, R., Prasad, M. A. J., Ungerbäck, J. & Sigvardsson, M. Transcription factor networks in B-cell differentiation link development to acute lymphoid leukemia. *Blood* **126,** 144–152 (2015).
101. Itoh-Nakadai, A. *et al.* The transcription repressors Bach2 and Bach1 promote B cell development by repressing the myeloid program. *Nat. Immunol.* **15,** 1171–1180 (2014).
102. Taylor, A. *et al.* SRF is required for neutrophil migration in response to inflammation. *Blood* **123,** 3027–3036 (2014).
103. Halene, S. *et al.* Serum response factor is an essential transcription factor in megakaryocytic maturation. *Blood* **116,** 1942–1950 (2010).
104. Smith, E. C. *et al.* MKL1 and MKL2 play redundant and crucial roles in megakaryocyte maturation and platelet formation. *Blood* **120,** 2317–2329 (2012).
105. Xu, Y. *et al.* A TFIID-SAGA Perturbation that Targets MYB and Suppresses Acute Myeloid Leukemia. *Cancer Cell* **33,** 13–28.e8 (2018).
106. Li, X. *et al.* Mammalian Polycomb-Like Pcl2/Mtf2 Is a Novel Regulatory Component of PRC2 That Can Differentially Modulate Polycomb Activity both at the Hox Gene Cluster and at Cdkn2a Genes. *Mol. Cell. Biol.* **31,** 351–364 (2011).
107. Shen, X. *et al.* Jumonji Modulates Polycomb Activity and Self-Renewal versus Differentiation of Stem Cells. *Cell* **139,** 1303–1314 (2009).
108. Lee, T. I. *et al.* Control of Developmental Regulators by Polycomb in Human Embryonic Stem Cells. *Cell* **125,** 301–313 (2006).
109. Wang, X. *et al.* Molecular analysis of PRC2 recruitment to DNA in chromatin and its inhibition by RNA. *Nat. Struct. Mol. Biol.* **24,** 1028–1038 (2017).